

Electronic Theses and Dissertations, 2004-2019

2005

An Investigation Of The Autoignition Of Power Generation Gas Turbine Fuel Blends Using A Design Of Experiments Approach

Jaap de Vries
University of Central Florida

 Part of the [Aerospace Engineering Commons](#)
Find similar works at: <https://stars.library.ucf.edu/etd>
University of Central Florida Libraries <http://library.ucf.edu>

This Masters Thesis (Open Access) is brought to you for free and open access by STARS. It has been accepted for inclusion in Electronic Theses and Dissertations, 2004-2019 by an authorized administrator of STARS. For more information, please contact STARS@ucf.edu.

STARS Citation

de Vries, Jaap, "An Investigation Of The Autoignition Of Power Generation Gas Turbine Fuel Blends Using A Design Of Experiments Approach" (2005). *Electronic Theses and Dissertations, 2004-2019*. 543.
<https://stars.library.ucf.edu/etd/543>

**AN INVESTIGATION OF THE AUTOIGNITION OF POWER GENERATION GAS
TURBINE FUEL BLENDS USING A DESIGN OF EXPERIMENTS APPROACH**

by

JAAP DE VRIES

B.S. College of Amsterdam (Hogeschool van Amsterdam), 2002

A thesis submitted in partial fulfillment of the requirements
for the degree of Master of Science
in the Department of Mechanical Material & Aerospace Engineering
in the College of Engineering and Computer Science
at the University of Central Florida
Orlando, Florida

Fall Term
2005

© 2005 Jaap de Vries

ABSTRACT

Natural gas has grown in popularity as a fuel for power generation gas turbines. However, changes in fuel composition are a topic of concern since fuel variability can have a great impact on the reliability and performance of the burner design. In particular, autoignition of the premixed fuel and air prior to entering the main burner is a potential concern when using exotic fuel blends. To obtain much-needed data in this area, autoignition experiments for a wide range of likely fuel blends containing CH₄ mixed with combinations of C₂H₆, C₃H₈, C₄H₁₀, C₅H₁₂, and H₂ were performed in a high-pressure shock tube. However, testing every possible fuel blend combination and interaction was not feasible within a reasonable time and cost. Therefore, to predict the surface response over the complete mixture domain, a special experimental design was developed to significantly reduce the amount of ‘trials’ needed from 243 to only 41 using the Box-Behnkin factorial design methodology. Kinetics modeling was used to obtain numerical results for this matrix of fuel blends, setting the conditions at a temperature of 800 K and pressure of 17 atm.

A further and successful attempt was made to reduce the 41-test matrix to a 21-test matrix. This was done using special mixture experimental techniques. The kinetics model was used to compare the smaller matrix to the expected results of the larger one. The new 21-test matrix produced a numerical correlation that agreed well with the results from the 41-test matrix, indicating that the smaller matrix would provide the same statistical information as the larger one with acceptable precision.

After the experimental matrix was developed using the design of experiments approach, the physical experiments were performed in the shock tube. Long test times were created by “tailoring” the shock tube using a novel driver gas mixture, obtaining test times of 10 millisecond or more, which made experiments at low temperatures possible.

Large discrepancies were found between the predicted results by numerical models and the actual experimental results. The main conclusion from the experiments is that the methane-based mixtures in this study enter a regime with a negative temperature coefficient when plotted in Arrhenius form. This means that these mixtures are far more likely to ignite under conditions frequently encountered in a premixer, potentially creating hazardous situations. The experimental results were correlated as a function of the different species. It was found that the effect of higher-order hydrocarbon addition to methane is not as profound as seen at higher temperatures (>1100 K). However, the ignition delay time could still be reduced by a factor two or more. It is therefore evident that potential autoignition could occur within the premixer, given the conditions as stated in this study.

To Marissa Selter

ACKNOWLEDGMENTS

Much I have learned from my advisor Dr Eric. L. Petersen.
I am grateful for all the help I got from my colleagues/co-students,
Joel M. Hall, Anothony Amadio, and Stefany L. Simmons.
Special thanks to Jack Selter.

TABLE OF CONTENTS

| | |
|---|------|
| LIST OF FIGURES | viii |
| LIST OF TABLES | xi |
| LIST OF SYMBOLS | xii |
| CHAPTER 1: INTRODUCTION | 1 |
| CHAPTER 2: BACKGROUND | 5 |
| 2.1 Combustion for power generation gas turbines | 5 |
| 2.2 Hydrocarbon combustion | 6 |
| CHAPTER 3: DESIGN OF EXPERIMENT | 13 |
| 3.1 Autoignition experiments | 13 |
| 3.2 Numerical model | 18 |
| 3.3 Reduced matrix | 21 |
| 3.4 Results | 30 |
| 3.5 Conclusions | 31 |
| CHAPTER 4: EXPERIMENTS | 35 |
| 4.1 Apparatus | 35 |
| 4.2 Mixtures | 39 |
| 4.3 Uncertainty analysis | 40 |
| 4.4 Shock-tube tailoring | 44 |
| 4.5 Results | 48 |
| CHAPTER 5: CONCLUSION AND RECOMMENDATIONS | 58 |
| 5.1 Conclusions | 58 |
| 5.2 Recommendations | 59 |
| APPENDIX A: PRESSURE AND EMISSION PLOTS FROM EXPERIMENT | 60 |
| LIST OF REFERENCES | 70 |

LIST OF FIGURES

| | |
|--|----|
| Figure 1: Energy used to generate electricity plotted by source over the last five decades [1]..... | 1 |
| Figure 2: Mixture space as used by Flores et al. [23]. Similar statistical techniques are employed in this study and can be found in Chapter 3..... | 9 |
| Figure 3: Typical NTC behavior as observed by Herzler et al. [29] for mixtures of n-heptane and air and pressures around 50 bar. | 11 |
| Figure 4: Correlation of autoignition times from numerical experiment using the 41-test matrix in Table 3. The correlation is of the form of Eqn. 1. | 17 |
| Figure 5: Chemical kinetics model prediction against experimental data [36]. | 18 |
| Figure 6: NTC behavior predicted by model for low temperature Ignition..... | 19 |
| Figure 7: Sensitivity analysis of the effect of hydrocarbon addition to methane on the ignition delay time. Sensitivity is as defined in Eqn. 2. | 21 |
| Figure 8: Constrained factor space for mixtures with 3 components [10]..... | 22 |
| Figure 9: Simplex Lattice design for 6 fuel components..... | 23 |
| Figure 10: Feasible mixture space with a lower bound on the methane mole fraction [10,13]. This is an example that employs only three mixture species..... | 24 |
| Figure 11: Experimental region for current study with upper bound for ethane and propane..... | 26 |
| Figure 12: Data compared against the quadratic polynomial, Eqn 8. This does not produce a good result..... | 28 |
| Figure 13: The exponential correlation obtained by the L21 matrix against data from L21..... | 29 |
| Figure 14: The correlation obtained by the L41 matrix applied to L21 levels. | 29 |

| | |
|---|----|
| Figure 15: Correlation from L21 against data from L41. | 31 |
| Figure 16: Plot of residuals against predicted values. The random scatter shows an unbiased or normal distribution of the residuals. From this one can conclude that a correlation of the form of Eqn. 1 creates a close to true response surface. | 32 |
| Figure 17: Schematic of the shock-tube facility used for the experiments. Only the lower shock tube was used herein [14]. | 36 |
| Figure 18: Schematic of the optical light detection system as employed in this study | 37 |
| Figure 19: velocity detection system. In this study only the last four velocity measurements were used [14]. | 39 |
| Figure 20: Linear fit through the four velocity measurements. Note that the distance z is the distance from the endwall and one is interested in the wave velocity at $z = 0$ | 42 |
| Figure 21: $x-t$ diagram for ‘tailored’ case. The contact surface remains stationary when $P_8 = P_5$. From Amadio et al. [44]. | 45 |
| Figure 22: Pressure trace for untailed and tailored conditions respectively. Note that test times of 14+ ms can be obtained by using a heavier driver gas. This case, He/CO ₂ 70/30% | 47 |
| Figure 23: Pressure and emission plot for a pure methane case (mix. 1) at 849 K. Note the gradual buildup of pressure and emission called ‘weak’ ignition. | 49 |
| Figure 24: Pressure and emission trace from a methane and pentane mixture (mix. 19). The steep pressure and emission rise due to ignition is called ‘strong’ ignition. | 49 |
| Figure 25: Parity plot for the experimental result against the correlation. | 52 |
| Figure 26: CH ₄ /H ₂ 75/25% Mixture (mix. 6) at 816 K. Note the weak ignition. | 54 |
| Figure 27: CH ₄ /H ₂ 50/50% Mixture (mix. 6) at 816 K. Note the strong ignition. | 54 |

Figure 28: CH₄ Data from this study compared against CH₄ data previously obtained. Note the shift in activation energy and the way the data connects..... 55

Figure 29: Data for pure CH₄ and mixtures both plotted against 10⁴/T. Two correlations are obtained for the two different cases..... 56

LIST OF TABLES

| | |
|--|----|
| Table 1: Fuel species with three levels each for auto ignition experiments. Petersen and de Vries [7]. | 13 |
| Table 2: Box-Behnkin 5-factor matrix for 3-level experiments as employed in L41 matrix by Petersen and de Vries [7]. | 14 |
| Table 3: Fractional factorial (41-test) matrix for the auto ignition experiments. Predictions by the model are provided | 16 |
| Table 4: The fuel compositions for the L21 (left) and converted pseudo components (right). | 26 |
| Table 5: Goodness of fit of different correlations all against data from L41. | 33 |
| Table 6: Experimental mixture table. The mixture numbers from the L21 can be found in the right column. | 40 |
| Table 7: Systematic and random uncertainties for the temperature (T_5) measurement. | 43 |
| Table 8: Mixture table with experimental result in ms. The prediction by the chemical kinetics model at 800 K is also given. Note the large difference in experimental results and the model predictions Model was evaluated at 800 K. | 50 |
| Table 9: Effect of amount of additive per species. | 52 |

LIST OF SYMBOLS

| | |
|----------------------|---|
| τ_{ign} | Ignition delay time, evaluated at the endwall |
| τ_{side} | Ignition delay time, evaluated at the sidewall |
| τ_{peak} | Peak time, evaluated at the sidewall |
| q | Integer number of different factors considered in an experiment |
| p | Number of level that are given per factor |

CHAPTER 1: INTRODUCTION

This Masters thesis concerns the autoignition of natural gas fuel blends used in the power generation gas turbine industry. Natural gas has increased in popularity as a fuel for electricity generation. While coal is still the main fuel used, it is estimated that 9 out of the next 10 power plants built will be using natural gas to fuel their power generation gas turbines [1]. A graphical presentation of the consumption for electricity generation by energy source can be found in Fig. 1.

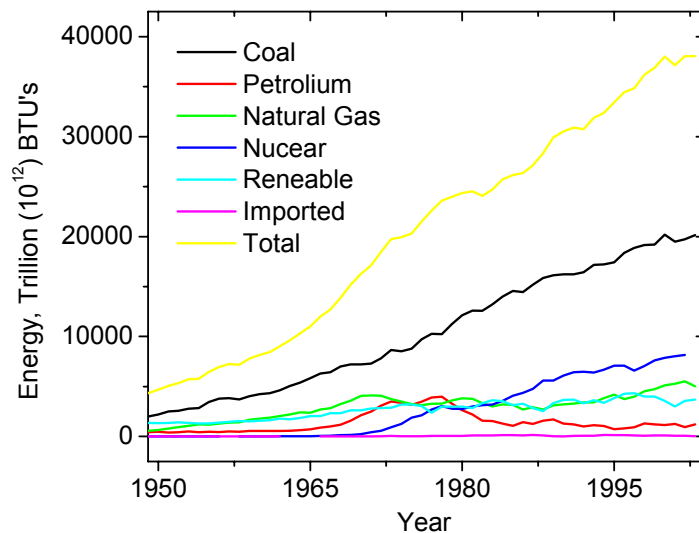


Figure 1: Energy used to generate electricity plotted by source over the last five decades [1].

A description of the operation of pre-mixed gas turbines, particularly their combustors, is given by Levebre [2]. Gas turbine engines operating on different combinations of hydrocarbon

fuels have been employed in the power generation industry as well as in the aero propulsion industry [2]. In both fields, restrictions with regard to pollutant formation have tightened in recent times due to regulations imposed by national as well as international authorities [3]. These restrictions have caused the industry to look at a wider variety of fuel blends. However, in the example of methane, used predominantly in the power generation industry in the form of natural gas, a small amount of a higher-order hydrocarbon impurity can cause dramatic changes in the burning characteristics of the overall fuel [4]. For example, additives such as a few percent ethane or propane can reduce the ignition delay time by a factor of two or more [5, 6]. This has a great impact on flame holding, stability, and reliability of the burner design. The effects of H₂ and higher-order hydrocarbon addition to natural gas on the performance of the gas turbines itself is not well known. The exact impact of significant (> 10%) levels of higher-order hydrocarbons in methane-based blends, much greater than typical impurity levels seen in natural gas, is also not known. Potential problems include flashback, premature ignition, combustion instability, and increased pollutant formation [7]. For this reason, the power generation industry would greatly benefit from knowing the burning characteristics of every possible combination of hydrocarbon that could be a constituent in the fuel; that is, having fundamental parameters such as ignition delay time and flame speed explicitly expressed as functions of the different constituents that could possibly make up the fuel.

Of particular concern to the study herein is the tendency of fuel blends to accelerate the ignition process relative to fuels containing predominantly methane. In the case of premixed combustors, the ignition delay time experienced with different fuel blends could actually be less than the residence time of the fuel-air mixtures inside the flame tubes feeding the combustor, causing premature ignition in the premixed circuits herein referred to as autoignition, or AI. The

conditions within the premixed circuit (upstream of the combustor) can be at temperatures between 600-800 K and pressures from 10 to 25 atm [8, 9]. For this reason, measurements of autoignition at typical operating conditions are needed over a wide range of possible fuel mixture compositions.

A problem such as this where the response or characteristic of a mixture is needed can be looked upon as posing a typical mixture problem [10]. The response of the experiments in this case would be the ignition delay time, τ_{ign} , which is a common measure of the oxidation kinetics. This characteristic time is a convenient parameter representing the chemical time scale and is often used to calibrate chemical kinetics models composed of the possible chemical reactions and their reaction rates [11]. However, testing the ignition delay time for every possible fuel combination would be very time consuming as well as costly in the sense that a lot of test gas and time would be needed to conduct all the experiments. Testing every possible combination would be the same as running a full factorial in which p^q amount of trials are needed. Here, q stands for the integer number of different factors, and p expresses the different levels at which these factors are tested.

Statistical Design of Experiments (DOE) techniques can possibly lead to smaller test matrices. These orthogonal, reduced matrices can generate outcomes similar to those of full factorial matrices [12]. The large number of factors involved in a thorough study on gas turbine fuel blend AI and oxidation chemistry make them ideal for utilizing DOE test matrices. There are many works in the literature that focus on experiments with mixtures [10, 13].

Chapter 3 presents the way reduced test matrices were developed for low-temperature, high-pressure autoignition experiments in shock tubes.

First, a 41-mixture matrix was developed using the DOE orthogonal matrix approach by Petersen and de Vries [7]. It ran in a numerical experiment with an improved chemistry model. Consecutively, the L41 matrix was reduced to an L21 assuming the response can be fitted with a second-order polynomial. Finally, a correlation of exponential form is derived from the L21 matrix. Details on the factors selected, AI trends, and the choices of experimental design are presented in chapter 3 on design of experiments.

All experiments in this study are performed at Dr. Eric Petersen's shock-tube facility located in El Segundo CA [14]. For several years, shock tubes have been utilized for the study of heterogeneous combustion processes. Shock tubes are useful for such measurements because a shock wave is capable of nearly instantaneously raising the temperature. A description of the shock tube is given in Chapter 4.

This thesis presents the results of a thorough investigation of the effect of fuel additives on the combustion of natural gas at low temperatures (800 K) and high pressures (20 atm). A background on the subject as well as similar studies performed in the past is given in Chapter 2. In this study, experimental design techniques are employed, minimizing the required number of experiments. A description of the methodology behind this experimental design is given in Chapter 3. Chapter 4 discusses the basic operation of a shock tube and the specific setup used in this study including an uncertainty estimate for the experimental results. Finally, a conclusion is given in Chapter 5, which also includes recommendations for future work.

CHAPTER 2: BACKGROUND

2.1 Combustion for power generation gas turbines

Developments in the art and science of gas turbine combustion have traditionally taken place gradually and continuously, and it is therefore hard to assign the success obtained over the years to one single person. A book frequently used by the author is “Gas Turbine Combustion” by Lefebvre [2]. This book focuses on the combustion of gas turbines used in the aviation as well as the power generation industry. It also takes into account the recent increase in public demand for more stringent regulations on pollutant emissions. The power generation gas turbines discussed here use lean-premixed combustion. Lean-premixed combustion is used because of its potential for ultra-low NO_x emissions. However, potential problems with lean premixed or “LPM” is the possibility for acoustic resonance. Also, the finite time necessary to achieve thorough mixing can exceed the autoignition delay time, causing premature ignition, and therefore dangerous conditions. Several studies have been conducted in order to characterize the combustion behavior of different hydrocarbons at conditions relevant to gas turbine combustion, with temperatures from 700-1500 K and pressures ranging from 10-50 atm. The next paragraph summarizes the studies that were deemed relevant to the current author’s investigation. The reader should keep in mind that this is not intended as an all-inclusive background in hydrocarbon combustion, since this would exceed the scope of the current study.

2.2 Hydrocarbon combustion

The literature on low-temperature (<1000K) shock-tube combustion is sparse. Conventional shock-tube operation allows test times in the order of one ms. Therefore testing the ignition behavior of fuel blends at lower temperature is usually not possible, since chemistry is slower and the reaction times fall outside the experimental range of the shock tube. The problem with test time limitation is overcome in this thesis by employing shock-tube tailoring, which is described in more detail in Chapter 4. As explained in Chapter 1, the autoignition of combustible mixtures can cause hazardous or at least undesirable conditions in the pre-mix circuit of power-generation gas turbines. Similar to gas turbines, internal combustion engines also deal with ignition problems, commonly referred to as engine knock. It is for this reason that several studies have been conducted on autoignition behavior of hydrocarbons. In 1993, Ciezki and Adomeit [15] investigated the autoignition of n-heptane-air mixtures under engine-relevant conditions using a high-pressure shock tube. The pressures were between 3.2 and 42 bar, the temperature varied between 660 and 1350 K, and equivalence ratios, the ratio between fuel/air divided by the perfect ratio of fuel/air, were between 0.5-3.0. Two different modes of ignition were detected, referred to as “strong” ignition and “weak” ignition. What “strong” and “weak” ignition is will be discussed in Chapter 4 and 5.

In 1997 Fieweger et al. [16] studied the self-ignition of several spark-ignition (SI) engine fuels (iso-octane, methanol, methyl ten-butyl ether and three different mixtures of iso-octane and n-heptane) mixed with air. This was done using the shock-tube technique under relevant engine conditions. NTC (negative temperature coefficient) behavior connected with a two-step (cool

flame) self-ignition at low temperatures was observed. This is an observation that agrees with the former study mentioned above and some of the current author's findings.

In 1998, Curran et al. developed a detailed chemical kinetics mechanism to be used for the study of oxidation of n-heptane in flow reactors, shock tubes, and rapid compression machines [17]. The validity range of the mechanism was for temperatures between 550-1700 K, pressure from 0-42 atm and equivalence ratios from 0.3-1.5. Data for jet-stirred reactors were used to refine the low-temperature portion of the reaction mechanism. Note that this study does not necessarily focus on the ignition behavior of n-heptane. However, the interest in this study is for every hydrocarbon of lower order than C_6 , which is found to be included in the heptane mechanism.

The most important component of natural gas studied herein is methane. An investigation on the ignition behavior of high-pressure methane was conducted by Petersen et al. in 1999 [18]. In this study, elevated pressures varied between 40-260 atm at low dilution levels. The temperature varied between 1040-1500 K. A new kinetic model was created based on the GRI-Mech 1.2.

The first study found by the author to mix natural gas with other fuel components was conducted in 2000 by Sierens and Rosseel [19]. In this study the effect of hydrogen addition to natural gas was investigated. The objective of this study was to lower the lean limit of combustion in order to get extremely low emission levels.

Following the detailed mechanism for n-heptane, Curran et al. created a mechanism for the oxidation of iso-octane mainly using the same techniques [20]. The iso-octane mechanism was validated over the same conditions as the n-heptane mechanism, using flow reactors and jet-stirred reactors to complement and refine the reactions at low and intermediate temperatures. This mechanism is of interest in this study because it exhibits phenomena like self-ignition, cool

flame, and negative temperature coefficient (NTC) behavior, similar to trends seen with the physical data in this study. For that reason, this mechanism was used to validate the experimental matrix as can be seen in Chapter 3.

In 2003, Lamoureux and Paillard studied the ignition delay times behind reflected shock waves for natural gas [21]. Their study was aimed at modeling the combustion behavior and to guarantee safe operation conditions when dealing with different types of natural gas. lamoureux's study emphasizes the point made in this study that the composition of natural gas can change drastically based upon its origin.

A shock-tube study in the ignition behavior of methane under engine-relevant conditions was conducted by Huang et al. [22]. The temperatures ranged from 1000 to 1350 K, and the pressure varied between 16-40 atm. Although this study was most relevant to internal combustion engine conditions, similar conditions are being experienced in gas turbines. The analytical study of methane oxidation was conducted using the detailed chemical kinetic mechanism as proposed by Petersen et al. [18].

Flores et al. investigated the impact of ethane and propane variation in natural gas on the performance of a model gas-turbine combustor [23]. In this study, an atmospherically fired model gas turbine combustor with a fuel flexible fuel/air premixer was employed to investigate the impact of significant amounts of ethane and propane addition into a baseline natural gas fuel supply. Similar to the current study, this study employed statistical experimental design methods, where mixture design methodology as described by Cornell [10] was combined with more traditional factorial designs. The response of interest in the study was the amount of NO_x and CO created when changing the particular fuel make-up.

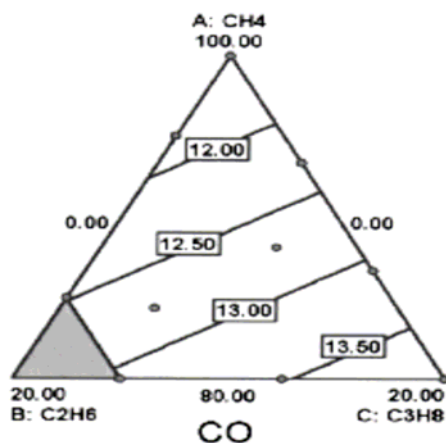


Figure 2: Mixture space as used by Flores et al. [23]. Similar statistical techniques are employed in this study and can be found in Chapter 3

Figure 1 shows a typical ternary plot generated in the study by Flores et al. [23]. Similar techniques are employed in the current study as can be seen in Chapter 3. The ethane/propane study was preceded by an investigation by Flores et al. in the combustor performance as a response to gaseous fuel variation [24].

In 2004 Bakali et al. conducted an experimental and modeling study of the oxidation of natural gas in premixed flames, shock tubes, and jet-stirred reactors [25]. This study discusses the fact that methane reactivity is significantly enhanced by higher hydrocarbons at low levels of concentration, resulting from the fact that heavy hydrocarbon radicals are more reactive than methyl (CH_3) radicals. The objective of the work was to validate a detailed reaction mechanism for the oxidation of natural gas taking into account the major and the minor alkanes that are present in the natural gas. Although Bakali's study does not cover the pressure range of this study (0.6 kPa), many similar conclusions are being drawn about the combustion characteristics of natural gas.

Gauthier et al. published a study about shock-tube determination of ignition delay times in fuel-blend and surrogate fuel mixtures [26]. This study supports the observation of a pronounced, low-temperature, NTC region similar to that experienced by Fieweger et al. [16] and in the current study.

Zhukov et al. (2004) investigated the autoignition behavior of n-pentane and air mixtures at temperatures from 867 to 1534 K and pressures from 11 to 530 atm [27]. Again this study shows a significant variation of the slope of the curve when plotted in arhennius form.

An interesting study of the combustion characteristics of a lower-order hydrocarbon (propane) was conducted by Herzler et al [28]. This was done under similar conditions as the current study with temperatures ranging from 900 to 1300 K and pressures of 10 and 30 bar. It is Herzler's observation that there is a shift in the activation energy around 1050 K making linear extrapolation not possible. In addition to the propane study, CCD pictures were made from the endwall location. These pictures show that the ignition takes place in the center of the shock tube. This is an important observation since the current study used light detection at the endwall to define the ignition delay time.

Another study by Herzler et al. focused on the shock ignition of n-heptane/air mixtures [29]. These were done using a shock tube creating conditions from 720 to 1100 K and pressures of about 50 bar.

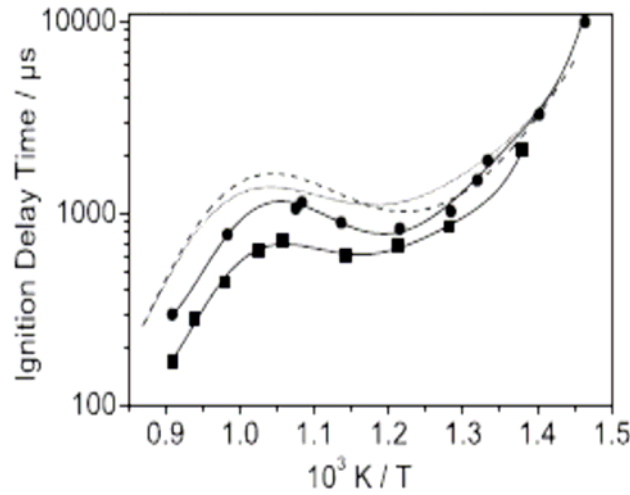


Figure 3: Typical NTC behavior as observed by Herzler et al. [29] for mixtures of *n*-heptane and air and pressures around 50 bar.

In addition to the familiar NTC behavior, the study showed a two-stage ignition at temperatures below 900 K. The negative temperature coefficient as observed by Herzler et al. [29] can be seen in Fig 2. This study used the chemical kinetics mechanism created by Curran et al. [17], which reproduced the general trends as observed experimentally. This is important since the model by Curran et al. is used in the current study for predicting non-linearities in the ignition behavior of natural gas fuel blends as can be read in Chapter 3.

In 2005, Buda et al. proposed a unified model for modeling the autoignition delay times of a wide range of alkanes [30]. The investigation conditions were temperatures from 600-1200 K and pressures from 1 to 50 bar. The model allows a satisfactory reproduction of ignition delay times obtained in a rapid compression machine or in a shock tube for *n*-pentane, iso-pentane, neo-pentane, 2-methylpentane, *n*-heptane, iso-octane, *n*-decane, and mixtures of *n*-heptane and iso-octane.

Finally, Huang and Bushe conducted an experimental and kinetic study of autoignition in methane/ethane/air and methane/propane/air mixtures under engine relevant conditions [31]. This was done using the reflected-shock technique at temperatures from 900 to 1400 K and pressures from 16 to 40 bar. A new model was developed showing reasonable agreement. It can be seen that there are several studies investigating the ignition behavior of fuel blends that are relevant in the current study. Most of these are tailored towards combustion in Internal Combustion (IC) engines or for Homogenously Charged Compression Ignition (HCCI) engines and focus on the pollutant formation such as NO_x or CO. However, several trends observed in these studies are relevant herein. First, the combustion behavior of higher-order hydrocarbons at lower temperatures found in former studies show a lot of similarities with the current author's findings, especially the NTC behavior at higher pressure and lower temperatures. Second, validation of a chemical kinetics mechanism as done in former studies under similar engine-relevant conditions justifies the use of such a model in the current study.

CHAPTER 3: DESIGN OF EXPERIMENT

3.1 Autoignition experiments

Possible fuel combinations dictate the range of autoignition experiments that are needed. The five different fuel species to be added to the base methane fuel are: ethane, propane, butane, pentane, and hydrogen. To minimize the number of experiments required to fully explore every possible fuel combination, three levels of each species were defined. Table 1 presents the three levels for the 5 fuel additives in terms of percentage of the fuel blend. Hence, a pure methane fuel will have a methane concentration of 100%. Even after assigning only 3 levels to each species, the total number of autoignition experiments required to test each possible combination would be 3^5 , or 243 different fuel blends. Reduced matrices that cover the same parameter space as the 243-blend full factorial matrix were considered and are discussed in Petersen and de Vries [7].

Table 1: Fuel species with three levels each for auto ignition experiments. Petersen and de Vries [7].

| Species | Levels (% of fuel) |
|-------------|--------------------|
| C_2H_6 | 0, 20, 40 |
| C_3H_8 | 0, 15, 30 |
| C_4H_{10} | 0, 10, 20 |
| C_5H_{12} | 0, 5, 10 |
| H_2 | 0, 10, 20 |

Design Of Experiment, (DOE) matrices specifically tailored for 3-level factors were derived by Box and Behnkin [32,33], and the appropriate matrix for a 5-factor experiment involves the 46-test matrix shown in Table 2. In the usual fashion, the three levels are assigned as 0, -1, and +1. When applying this nomenclature to the Table 1 concentration levels, the 0 value corresponds to the zero % level; the -1 corresponds to the middle level; and the +1 level corresponds to the largest concentration. The complete fuel-blend autoignition matrix is provided as Table 3. Each entry in the table contains the appropriate % level of that species, where the baseline combination has all zeros and corresponds to the fuel being pure methane. Provided in Table 3 as an extra column is the CH₄ fraction; note that this is not actually one of the main 5 factors in the matrix. Rather, the CH₄ concentration is a result of assigning levels to the other fuel species that are in the DOE matrix.

Table 2: Box-Behnkin 5-factor matrix for 3-level experiments as employed in L41 matrix by Petersen and de Vries [7].

| Factors | | | | |
|---------|----|----|----|----|
| A | B | C | D | E |
| ±1 | ±1 | 0 | 0 | 0 |
| 0 | 0 | ±1 | ±1 | 0 |
| 0 | ±1 | 0 | 0 | ±1 |
| ±1 | 0 | ±1 | 0 | 0 |
| 0 | 0 | 0 | ±1 | ±1 |
| 0 | 0 | 0 | 0 | 0 |
| 0 | ±1 | ±1 | 0 | 0 |
| ±1 | 0 | 0 | ±1 | 0 |
| 0 | 0 | ±1 | 0 | ±1 |
| ±1 | 0 | 0 | 0 | ±1 |
| 0 | ±1 | 0 | ±1 | 0 |
| 0 | 0 | 0 | 0 | 0 |

(x3)

(x3)

A thermochemical equilibrium code (STANJAN) was employed for calculating the equivalence ratio to produce a typical burner adiabatic flame temperature. The results led to the fact that ϕ actually varies less than a few percent amongst all 41 blends to attain the same combustor adiabatic flame temperature for typical conditions (1400 K, 17 atm). Hence, for simplicity, the same ϕ was assigned to each fuel/air mixture using the fuel blends in Table 3, specifically $\phi = 0.5$. A numerical exercise was performed using the Table 3 blends, and the autoignition conditions to reproduce the results as if they were performed in the laboratory. This exercise was undertaken to produce results from the 41-test matrix that could be correlated. The main purpose of the correlation was that it could then be used to represent the autoignition results over the parameter space defined by the five factors and the experimental constants (ϕ , P).

As discussed in the next section, the correlation was used to determine whether or not a smaller matrix that has fewer fuel combinations produces the same autoignition results. This numerical experiment required a chemical kinetics model to obtain the predicted ignition times. The Lawrence Livermore Mechanism [20] with the heptane chemistry included was selected for the calculations mainly because it is based on a core methane oxidation model and has extensive chemistry for the higher-order hydrocarbons (for convenience in performing multiple calculations). The *Chemkin* suite of software was used to run the mechanism, utilizing the shock module to match what would happen in a shock-tube experiment [34]. The Lawrence Livermore mechanism was designed for the lower temperatures (800 – 1000 K) of the auto ignition study; reproducing the correct ignition delay times per se was secondary to obtaining results that were realistic and self-consistent from blend to blend. Shown in Table 3 in the last column are the numerical results for the autoignition case.

Table 3: Fractional factorial (41-test) matrix for the auto ignition experiments. Predictions by the model are provided

| Mix | Fuel Blend Components (%) | | | | | | τ_{ign} (s) |
|-----|---------------------------|-------------------------------|-------------------------------|--------------------------------|--------------------------------|----------------|-------------------------|
| | CH ₄ | C ₂ H ₆ | C ₃ H ₈ | C ₄ H ₁₀ | C ₅ H ₁₂ | H ₂ | |
| 1 | 100 | 0 | 0 | 0 | 0 | 0 | 1.71 |
| 2 | 65 | 20 | 15 | 0 | 0 | 0 | 0.91 |
| 3 | 50 | 20 | 30 | 0 | 0 | 0 | 0.71 |
| 4 | 45 | 40 | 15 | 0 | 0 | 0 | 1.02 |
| 5 | 30 | 40 | 30 | 0 | 0 | 0 | 0.8 |
| 6 | 85 | 0 | 0 | 10 | 5 | 0 | 0.059 |
| 7 | 80 | 0 | 0 | 10 | 10 | 0 | 0.038 |
| 8 | 75 | 0 | 0 | 20 | 5 | 0 | 0.036 |
| 9 | 70 | 0 | 0 | 20 | 10 | 0 | 0.028 |
| 10 | 75 | 0 | 15 | 0 | 0 | 10 | 0.75 |
| 11 | 65 | 0 | 15 | 0 | 0 | 20 | 0.76 |
| 12 | 60 | 0 | 30 | 0 | 0 | 10 | 0.6 |
| 13 | 50 | 0 | 30 | 0 | 0 | 20 | 0.6 |
| 14 | 70 | 20 | 0 | 10 | 0 | 0 | 0.209 |
| 15 | 60 | 20 | 0 | 20 | 0 | 0 | 0.087 |
| 16 | 50 | 40 | 0 | 10 | 0 | 0 | 0.269 |
| 17 | 40 | 40 | 0 | 20 | 0 | 0 | 0.11 |
| 18 | 85 | 0 | 0 | 0 | 5 | 10 | 0.118 |
| 19 | 75 | 0 | 0 | 0 | 5 | 20 | 0.114 |
| 20 | 80 | 0 | 0 | 0 | 10 | 10 | 0.048 |
| 21 | 70 | 0 | 0 | 0 | 10 | 20 | 0.046 |
| 22 | 75 | 0 | 15 | 10 | 0 | 0 | 0.131 |
| 23 | 65 | 0 | 15 | 20 | 0 | 0 | 0.06 |
| 24 | 60 | 0 | 30 | 10 | 0 | 0 | 0.162 |
| 25 | 50 | 0 | 30 | 20 | 0 | 0 | 0.079 |
| 26 | 75 | 20 | 0 | 0 | 5 | 0 | 0.228 |
| 27 | 70 | 20 | 0 | 0 | 10 | 0 | 0.09 |
| 28 | 55 | 40 | 0 | 0 | 5 | 0 | 0.35 |
| 29 | 50 | 40 | 0 | 0 | 10 | 0 | 0.147 |
| 30 | 80 | 0 | 0 | 10 | 0 | 10 | 0.089 |
| 31 | 70 | 0 | 0 | 10 | 0 | 20 | 0.087 |
| 32 | 70 | 0 | 0 | 20 | 0 | 10 | 0.04 |
| 33 | 60 | 0 | 0 | 20 | 0 | 20 | 0.038 |
| 34 | 70 | 20 | 0 | 0 | 0 | 10 | 1.53 |
| 35 | 60 | 20 | 0 | 0 | 0 | 20 | 1.61 |
| 36 | 50 | 40 | 0 | 0 | 0 | 10 | 1.6 |
| 37 | 40 | 40 | 0 | 0 | 0 | 20 | 1.63 |
| 38 | 80 | 0 | 15 | 0 | 5 | 0 | 0.167 |
| 39 | 75 | 0 | 15 | 0 | 10 | 0 | 0.075 |
| 40 | 65 | 0 | 30 | 0 | 5 | 0 | 0.202 |
| 41 | 60 | 0 | 30 | 0 | 10 | 0 | 0.103 |

Autoignition times (τ_{AI}) at 800 K and 17 atm could be correlated by an expression of the form:

$$\tau_{AI} = A \prod_i (1 - 10 \cdot x_i)^{n_i} \quad (1)$$

where A is a constant, and x_i is the mole fraction of fuel species i in the blend. A correlation involving species concentrations raised to an exponent was selected as the form of the autoignition time relation herein because similar forms have been employed by many investigators to correlate their ignition delay times [35]. The resulting correlation in comparison with the autoignition-time results of the 41-test matrix is presented on a parity plot in Fig. 1. The correlation has an r^2 value of 0.978 and is assumed to adequately reproduce the trends from the autoignition numerical exercise.

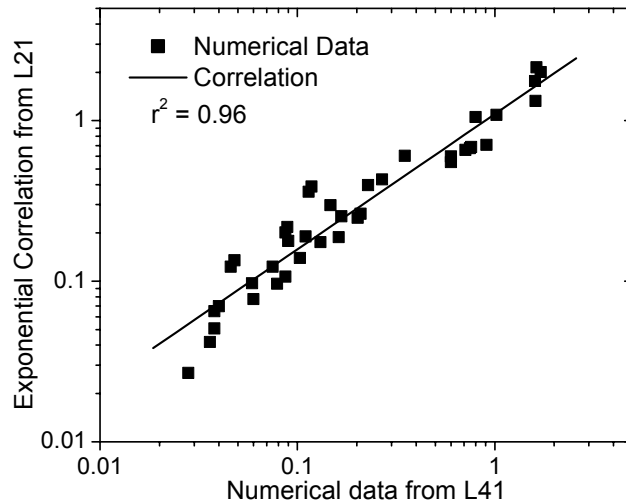


Figure 4: Correlation of autoignition times from numerical experiment using the 41-test matrix in Table 3. The correlation is of the form of Eqn. 1.

3.2 Numerical model

As discussed in the last section, a numerical model was employed to give a prediction of the possible ignition delay times for different mixtures. The chemical kinetics mechanism created by the Lawrence Livermore National Laboratory was used in this case since it includes all the chemistry necessary for these experiments. Shock-tube measurements at low temperatures (800 K) and at gas turbine pressures (17 atm) are extremely rare. Therefore, the model is not expected to agree well with the data to be found. However, the model should predict chemical nonlinearities that are specific to combustion chemistry and fuel blending. Therefore, a good correlation through the modeling data would indicate that the same type of correlation would serve well with real physical data. The behavior of the chemical kinetics mechanism can be seen in Fig. 2, which shows the prediction from the Lawrence Livermore mechanism against data presented earlier by the authors [36], but at temperatures above 1000 K.

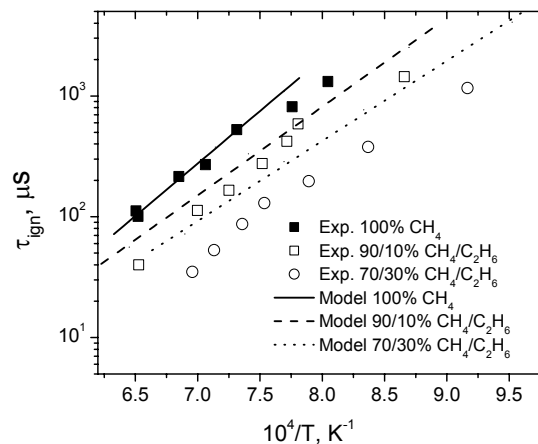


Figure 5: Chemical kinetics model prediction against experimental data [36].

It can be seen in Fig. 2 that the model starts overpredicting the data when larger percentages of higher-order hydrocarbons are added. Yet, the slope of the model seems to agree well with the slope that is given by experiments. One can see that the model has the tendency to over predict the experimental data, especially when higher-order hydrocarbons are added.

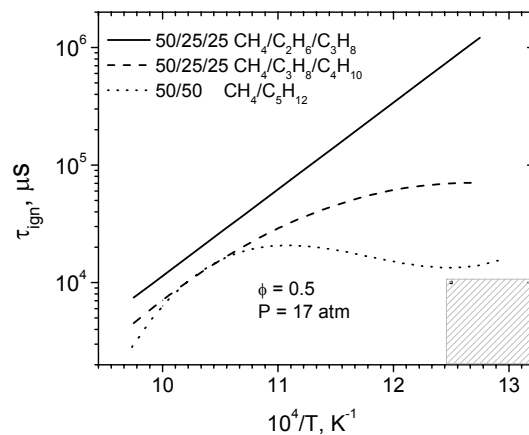


Figure 6: NTC behavior predicted by model for low temperature Ignition.

Figure 3 shows the model's prediction at lower temperatures. Note that at these temperatures and pressures, there are no experimental data yet available. It can be clearly seen in Fig. 3 that the addition of higher-order hydrocarbons greatly accelerates the ignition process. The regime that is hatched in the lower right corner of Fig. 3 is the region where autoignition is likely to occur in the gas turbine's premixer. The model shows that addition of pentane with methane gives ignition times that come dangerously close to this unwanted regime. This becomes particularly evident when one remembers from Fig. 2 that the model has the tendency to overpredict the experimental data. Another interesting observation is the negative temperature coefficient

(NTC) effect that the mixture with pentane shows between 800 and 900 K. This NTC behavior leads to ignition times that are much smaller at lower temperatures than what might be extrapolated from data and models based exclusively on higher-temperature (and lower-pressure) behavior. It would be helpful to know which fuel component has the strongest effect on the acceleration of ignition of methane-based fuel blends. To quantify this, a sensitivity analysis was conducted using the correlation obtained from the chemical kinetics model. The sensitivity can be obtained by taking the partial derivative of this correlation with respect to each of the additional fuel components, such that

$$\left. \frac{\partial \tau_{ign}(\chi_i)}{\partial \chi_i} \right|_{\chi_{CH_4}=100\%} \quad (2)$$

where ‘i’ stands for methane, ethane.....hydrogen, i.e. the species that can be found in Table 1. The result of this sensitivity analysis can be found in Fig. 4. The numerical model predicts that the addition of Pentane has the strongest effect on the ignition delay time. It also shows that the effect reduces when the order of the additional hydrocarbon goes down. Surprisingly, the effect of the addition of hydrogen is marginal, as shown in Fig. 4.

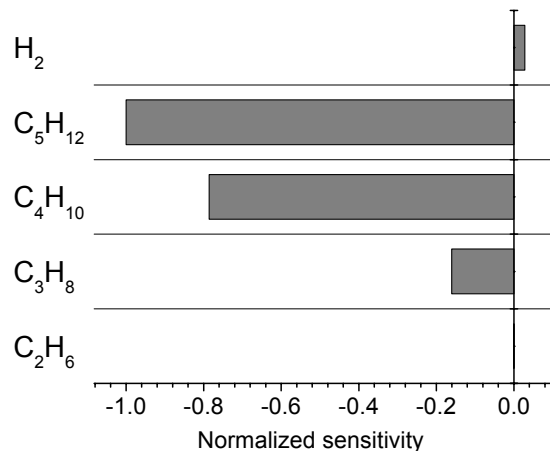


Figure 7: Sensitivity analysis of the effect of hydrocarbon addition to methane on the ignition delay time. Sensitivity is as defined in Eqn. 2.

3.3 Reduced matrix

The large matrix design has proven to give a satisfactory fit of the numerical data. However, conducting experiments using 41 different mixtures is still a quite elaborate process and, if possible, further reduction of the matrix would be desirable. In the response surface obtained using the Box-Behnkin method such as the 41-test matrix obtained above, the levels chosen are independent of the levels chosen for the other factors. In a mixture experiment, the factors are the ingredients or components of the mixture, and the response is a function of the proportions of each ingredient, which are typically measured by weight, volume, or molar ratios. The summation of all the components has to reach unity, which causes the individual levels of the factors to be dependent.

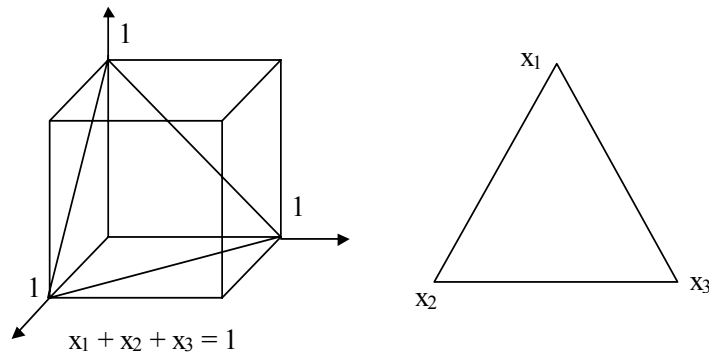


Figure 8: Constrained factor space for mixtures with 3 components [10].

This is what makes mixture experiments different from the usual response surface experiments [10,13]. Mixture compositions can be either pure, binary, tertiary, etc., depending upon how many different components are included. A mixture that includes all possible components is called a complete mixture. The proportion of a mixture can be graphically represented using a simplex coordinate system. An example is given in Fig. 5 for $q = 3$ components. Each of the three vertices in the equilateral triangle corresponds to a pure blend, and the sides are made up of binary blends. For more on mixture experiments, the reader is strongly advised to read Cornell [10]. Mixture problems are very common in the chemical or food industry. The two main designs using simplexes are the simplex lattice design and the simplex-centroid design. A simplex lattice design is just a uniformly spaced set of points on a simplex. The number of points on each side of the simplex is given by the order of the polynomial that one would like to fit. In a simplex-centroid design, all levels are equal in value or 0 otherwise, $(1,0,0,0)$, $(1/2,1/2,0,0)$, $(1/3,1/3,1/3,0)$, etc. Simplex-centroid designs are often used when it is expected that cubic terms might be necessary

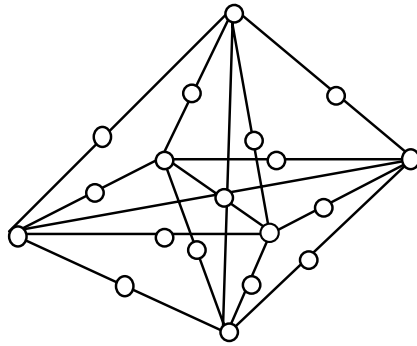


Figure 9: Simplex Lattice design for 6 fuel components.

Figure 6 shows a simplex lattice design for the current problem in 3-D designed to fit a second-order polynomial. Notice that all the corners (vertices) represent pure mixtures. However, when investigating methane-based fuel blends, it is very unlikely that the mole fraction of methane becomes less than 50%. In other words, there are constraints on the component proportions that prevent one from exploring the entire simplex region. Only a sub region of the simplex shown in Fig. 7 is relevant for the current study.

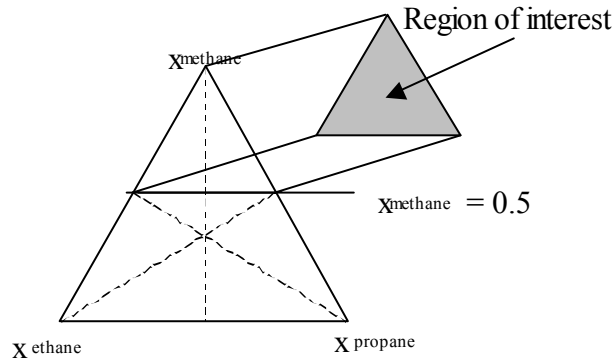


Figure 10: Feasible mixture space with a lower bound on the methane mole fraction [10,13]. This is an example that employs only three mixture species.

The general form of the constrained mixture problem is

$$\sum_{i=1}^q x_i \equiv 1 \quad (3)$$

$$L_i \leq x_i \leq U_i \quad (4)$$

where L_i stands for the lower bound and U_i for the upper bound. All the upper-bound limits for the fuels are given in Table 1. The effect of the upper and lower bound restrictions in Eqn. 4 is to limit the feasible space for the mixture experiment to a sub region of the simplex. For illustrative purposes, a triangular simplex is used to graphically represent the design process. (However, the reader should be aware that the simplex including all components (Hydrocarbons) actually takes the form of Fig. 8.) When one component has a lower limit L_i , then the maximum value that any other components could reach would be $U_{j \neq i} = 1 - L_i$. If only methane is bounded and the other

components simply have an upper bound of $U_i = 1 - L_{\text{methane}}$, then the feasible experimental region is as seen in Fig. 7, in which only ethane and propane are shown for illustrative purposes.

In the case of Fig. 7, the experimental region is still a simplex, and it seems reasonable to define a new set of components that will take on the values 0 to 1 over the feasible region. The redefined components are called L-pseudo components, or just pseudo components. The pseudo components X_i are defined using the transformation

$$X_i = \frac{x_i - L_i}{1 - L} \quad (5)$$

$$L = \sum_{i=1}^q L_i < 1 \quad (6)$$

It is recommended that the pseudo components be used to fit the mixture model. This is because constrained design spaces usually have high levels of multicollinearity or ill conditioning [13]. The reduced simplex method described above assumes that the only constraint is the lower bound constraint on methane.

In fact, as can be seen in Table 1, the additional proportions of the other hydrocarbons all have different upper bounds. This leads to an experimental region that is not a simplex as can be seen in Fig. 8. In such cases computer generated designs, such as the D-optimal algorithm are logical design alternatives.

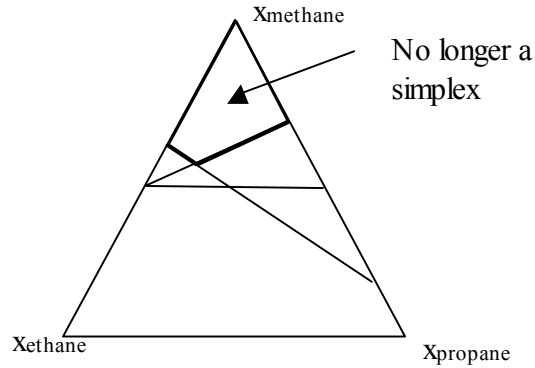


Figure 11: Experimental region for current study with upper bound for ethane and propane.

Table 4: The fuel compositions for the L21 (left) and converted pseudo components (right).

| mix# | Original Fuel blend components (%) | | | | | | tign (s) | Pseudo components | | | | | |
|------|------------------------------------|-------------------|-------------------|--------------------|--------------------|-----------------|----------|-------------------|-------------------|-------------------|--------------------|--------------------|-----------------|
| | X _{ch4} | X _{c2h6} | X _{c3h8} | X _{c4h10} | X _{c5h12} | X _{h2} | | X _{ch4} | X _{c2h6} | X _{c3h8} | X _{c4h10} | X _{c5h12} | X _{h2} |
| 1 | 100 | 0 | 0 | 0 | 0 | 0 | 1.71 | 1 | 0 | 0 | 0 | 0 | 0 |
| 2 | 75 | 25 | 0 | 0 | 0 | 0 | 1.65 | 0.5 | 0.5 | 0 | 0 | 0 | 0 |
| 3 | 75 | 0 | 25 | 0 | 0 | 0 | 0.63 | 0.5 | 0 | 0.5 | 0 | 0 | 0 |
| 4 | 75 | 0 | 0 | 25 | 0 | 0 | 0.042 | 0.5 | 0 | 0 | 0.5 | 0 | 0 |
| 5 | 75 | 0 | 0 | 0 | 25 | 0 | 0.024 | 0.5 | 0 | 0 | 0 | 0.5 | 0 |
| 6 | 75 | 0 | 0 | 0 | 0 | 25 | 2.31 | 0.5 | 0 | 0 | 0 | 0 | 0.5 |
| 7 | 50 | 50 | 0 | 0 | 0 | 0 | 1.77 | 0 | 1 | 0 | 0 | 0 | 0 |
| 8 | 50 | 25 | 25 | 0 | 0 | 0 | 0.79 | 0 | 0.5 | 0.5 | 0 | 0 | 0 |
| 9 | 50 | 25 | 0 | 25 | 0 | 0 | 0.073 | 0 | 0.5 | 0 | 0.5 | 0 | 0 |
| 10 | 50 | 25 | 0 | 0 | 25 | 0 | 0.036 | 0 | 0.5 | 0 | 0 | 0.5 | 0 |
| 11 | 50 | 25 | 0 | 0 | 0 | 25 | 1.82 | 0 | 0.5 | 0 | 0 | 0 | 0.5 |
| 12 | 50 | 0 | 50 | 0 | 0 | 0 | 0.52 | 0 | 0 | 1 | 0 | 0 | 0 |
| 13 | 50 | 0 | 25 | 25 | 0 | 0 | 0.071 | 0 | 0 | 0.5 | 0.5 | 0 | 0 |
| 14 | 50 | 0 | 25 | 0 | 25 | 0 | 0.037 | 0 | 0 | 0.5 | 0 | 0.5 | 0 |
| 15 | 50 | 0 | 25 | 0 | 0 | 25 | 0.64 | 0 | 0 | 0.5 | 0 | 0 | 0.5 |
| 16 | 50 | 0 | 0 | 50 | 0 | 0 | 0.023 | 0 | 0 | 0 | 1 | 0 | 0 |
| 17 | 50 | 0 | 0 | 25 | 25 | 0 | 0.017 | 0 | 0 | 0 | 0.5 | 0.5 | 0 |
| 18 | 50 | 0 | 0 | 25 | 0 | 25 | 0.038 | 0 | 0 | 0 | 0.5 | 0 | 0.5 |
| 19 | 50 | 0 | 0 | 0 | 50 | 0 | 0.013 | 0 | 0 | 0 | 0 | 1 | 0 |
| 20 | 50 | 0 | 0 | 0 | 25 | 25 | 0.021 | 0 | 0 | 0 | 0 | 0.5 | 0.5 |
| 21 | 50 | 0 | 0 | 0 | 0 | 50 | 2.8 | 0 | 0 | 0 | 0 | 0 | 1 |

Another alternative is to have all non-methane fuel components vary between 0 and 40%. That way the only restriction is the lower limit of methane and a reduced simplex such as shown in

Fig. 7 can be employed using L-pseudo components. However, making all other fuel components divert from the original region of interest can cause larger errors in the final correlation. Table 4 shows the design for a quadratic polynomial presented in the original component proportions and also in pseudo components. The simplex lattice experimental design as seen in Table 4 is used to find a second-order polynomial.

The dependence between the components, see Eqn. 3, can be used to simplify the polynomial model that can be fitted through the experimental data. One method is substituting Eqn. 7 in the polynomial.

$$X_q = 1 - \sum_{i=1}^{q-1} X_i \quad (7)$$

This is just Eqn. 3 written in a different form. This approach is not widely accepted because it obscures the effect of the q^{th} component. Another form is a method described in great detail by Cornell [10]. It produces the general second-order polynomial

$$\eta = \beta_0 + \sum_{i=1}^q \beta_i X_i + \sum_{i \leq j}^q \sum_j^q \beta_{ij} X_i X_j \quad (8)$$

Into the form

$$\eta = \sum_{i=1}^q \beta'_i X_i + \sum_{i < j}^q \sum_j^q \beta'_{ij} X_i X_j \quad (9)$$

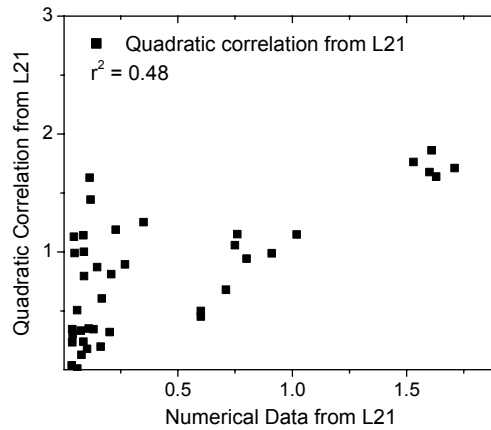


Figure 12: Data compared against the quadratic polynomial, Eqn 8. This does not produce a good result.

This form is also called canonical or Scheffé form. Note that here X is used instead of x which means that the polynomials will correlate the pseudo components. For the case here, $q = 6$, and Eqn. 7 will have 21 coefficients, just as many as there are trials in the matrix in Table 4. There are 21 equations and 21 unknowns. This means that every coefficient can uniquely be solved for this problem. The $\beta_{ij}X_iX_j$ Terms present the excess response from the quadratic model over the linear model. This is often called synergism or antagonism due to nonlinear blending. The quadratic model such as Eqn. 9 has the advantage that the interaction between every component becomes evident. The model used for Eqn. 1 takes into account higher-order interactions. This can be clearly seen in the L41 matrix where several components are included per trial, and the matrix is less sparsely populated than the matrix in Table 4.

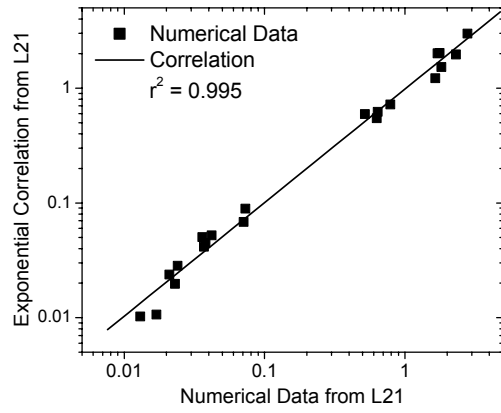


Figure 13: The exponential correlation obtained by the L21 matrix against data from L21.

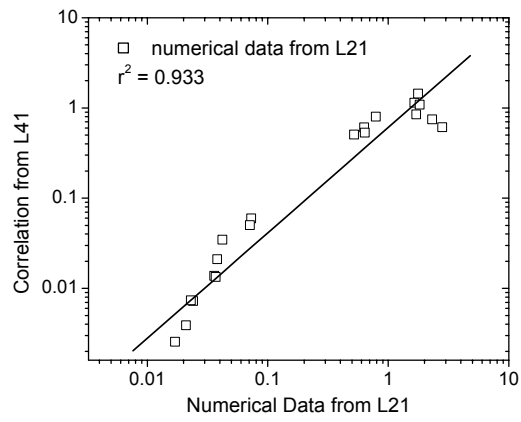


Figure 14: The correlation obtained by the L41 matrix applied to L21 levels.

3.4 Results

To test the result obtained using the simplex lattice method, the correlation was tested against the L41 matrix. An analysis of variance (ANOVA) was conducted going both ways. First, it is very likely that in practice mixtures will be used that are just binary blends. For that reason the correlation found using the Box-Behnkin method should give a good fit through the data that were obtained using the L21 in Fig 4. Vice versa, the second-order polynomial obtained with the simplex lattice method should be verified against the L41 matrix. It becomes clear from analyzing Fig. 9 that the quadratic correlation obtained from the simplex lattice design does not agree well with the numerical data obtained for the L41. Figure 11 shows the correlation obtained from the L41 to correlate the compositions from the L21 matrix. It is clear that the agreement is satisfactory and that the L41 can properly be used to create a suitable response surface, as expected. It also follows from the high r^2 value from the correlation in the form of Eqn. 1 that an exponential correlation must come close to describing the real response surface. It is therefore a logical step to find a similar response using the L21 matrix. Thus, instead of trying to fit a second-order polynomial, a correlation of the form of Eqn. 1 was attempted. The result is shown in Fig. 12, which shows clearly that the natural response surface must come close to that in the form of Eqn. 1, which is what one would expect from the underlying physics.

The last question that needs to be asked is if the exponential correlation obtained from the L21 will predict a good agreement with the numerical results obtained from the L41. If so, the correlation is tested over a wide range of fuel blends, and a strong argument can be raised to further reduce the L41 test matrix to a L21. Such a comparison can be seen in Fig. 12. The r^2 of the result in Fig. 12 turns out to be 0.96 when tested over the full factorial range. Therefore, it

appears that the L21 matrix can be used in lieu of the larger L41 matrix yet produce the same trend.

It is always necessary to examine the predicted model to ensure that it provides an adequate approximation to the true system, also called ANalysis Of VAriance, or ANOVA. One check is the residual analysis where $e_i = y_i - \hat{y}_i$ is the residual from the least squares fit. When e_i (%) is plotted against \hat{y}_i , which can be seen in Fig. 13, a random distribution or scatter suggests that the variance of the original observation is constant for all values of y_i , and that the correlation is unbiased. When analyzing Fig. 13 it can be concluded that the predicted response is unbiased with respect to the value of y . In Table 5 the results obtained from different correlations are summarized. All correlations are compared against the L41 test matrix.

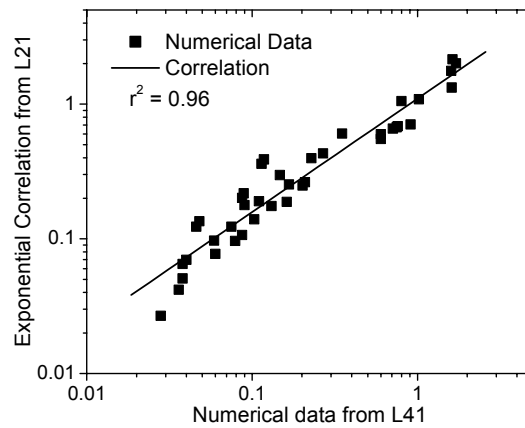


Figure 15: Correlation from L21 against data from L41.

3.5 Conclusions

Performing a comprehensive set of shock-tube ignition experiments over a wide range of possible fuel blends can be a daunting task, particularly when the blend may contain a mixture of

methane with as many as five other species, each having volumetric mole fractions greater than 5%. The mixture experimental matrix derived herein provides an alternative to performing ignition experiments for all possible fuel combinations. Since the data to be generated from the experiments serve a specific purpose—that is, the determination as to whether a given mixture will ignite within a time frame of 10 ms at 800 K and 17 atm—such a matrix provides an effective way to obtain such data in a limited time frame for immediate application by the gas turbine industry.

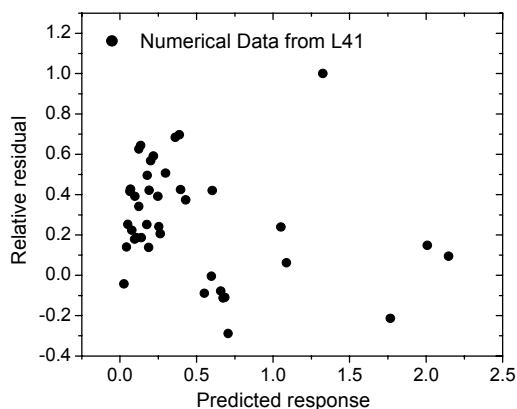


Figure 16: Plot of residuals against predicted values. The random scatter shows an unbiased or normal distribution of the residuals. From this one can conclude that a correlation of the form of Eqn. 1 creates a close to true response surface.

For some mixtures, as predicted by the chemical kinetics model in Table 3, the expected ignition time might be outside the 10-15 ms time frame of the shock-tube experiment itself. Even though such an experiment would not provide an actual ignition delay time, it still would provide useful information from a “safe” or “unsafe” standpoint with regard to premixing that fuel with

air prior to entering the burner of a power generation gas turbine engine. It is worth mentioning again that the τ_{ign} predictions from the kinetics model in Tables 3 and 4 should be used only for comparing the L21 and L41 results and are not replacements for actual data due to the lack of validation for this (and other) kinetics mechanisms at gas turbine conditions at present. The trends from recent high-pressure data indicate that the model may overpredict τ_{ign} .

Table 5: Goodness of fit of different correlations all against data from L41.

| Matrix used for correlation | Correlation | r^2 |
|-----------------------------|-------------|-------|
| L21 | Quadratic | 0.48 |
| L41 | Exponential | 0.98 |
| L21 | Exponential | 0.96 |

When performing the shock-tube experiments for the 21 fuel blends in Table 4, the authors anticipate conducting more experiments than the number implied by the matrix. For example, a given blend may not produce quantitative data within the time frame of the experiment, as previously mentioned, so additional tests at higher temperatures will be performed to determine what temperature is required for a given fuel/air mixture to ignite in less than 10 ms. Also of concern to the gas turbine industry are fuel/air mixtures with equivalence ratios of 1.0, which, according to kinetics models, should be more likely to ignite than the $\phi = 0.5$ mixtures of interest herein. Stoichiometric mixtures can also be explored using the fuel-blend matrices in this paper. Additional experiments beyond those implied by the test matrices are also required to provide further insight into the complex chemical kinetics of CH_4 -based fuel blends. Other DOE-based matrices for such experiments are suggested by Petersen and de Vries [4].

Finally, it should be noted that although the primary application is one concerning a set of shock-tube autoignition experiments at a specific temperature, pressure, and fuel/air equivalence ratio, the mixture matrix could also be employed in other experiments in need of combustion data for the same range of mixture combinations. For example, the L21 (or L41) matrix can be used to guide a series of flame speed experiments where the primary result is a measured flame speed for a given initial mixture of air and fuel blend. The matrix can also be used to study ignition for the same range of fuel combinations in apparatuses such as flow reactors and rapid compression devices.

CHAPTER 4: EXPERIMENTS

4.1 Apparatus

A significant aspect of the design of a gas turbine combustor is the time-dependent interaction of the species within the high temperature combustion zone, or as in the case in this thesis, a region outside the designed combustion zone where combustion could take place, whether intentionally or non-intentionally. Chemical kinetics is one of the fundamental topics of importance during the design phase of a combustor. Because of their highly repeatable test conditions and uniform flow fields, shock tubes have been used for several decades to study these topics [14]. Details about general shock tube usage for gas-phase combustion experiments can be found in Bowman and Hanson [37], Glass and Sislán [38], and Bhaskaran and Roth [39]. Shock tubes are useful for measurements of heterogeneous combustion processes because the shock wave can be used to heat the mixture nearly instantaneously to temperatures on the order of 700 to 4000 K in a controlled environment. In the present application, the shock-tube technique is utilized for the study of low-temperature reaction times of gas turbine fuel blends as well as time histories of CH* emissions. The emission together with the pressure profiles are useful to detect “strong” or “weak” ignition in addition to the ignition time itself. The facility used in the present study is located at the Aerospace Corporation in El Segundo CA, and a wide-ranging description of this shock tube is given by Petersen et al [14]. In addition to the main shock-tube hardware, this facility includes a vacuum system, a velocity detection system, an optical detection system, and a

data acquisition system. A schematic of the shock tube and its gas-handling system can be found in Fig. 17.

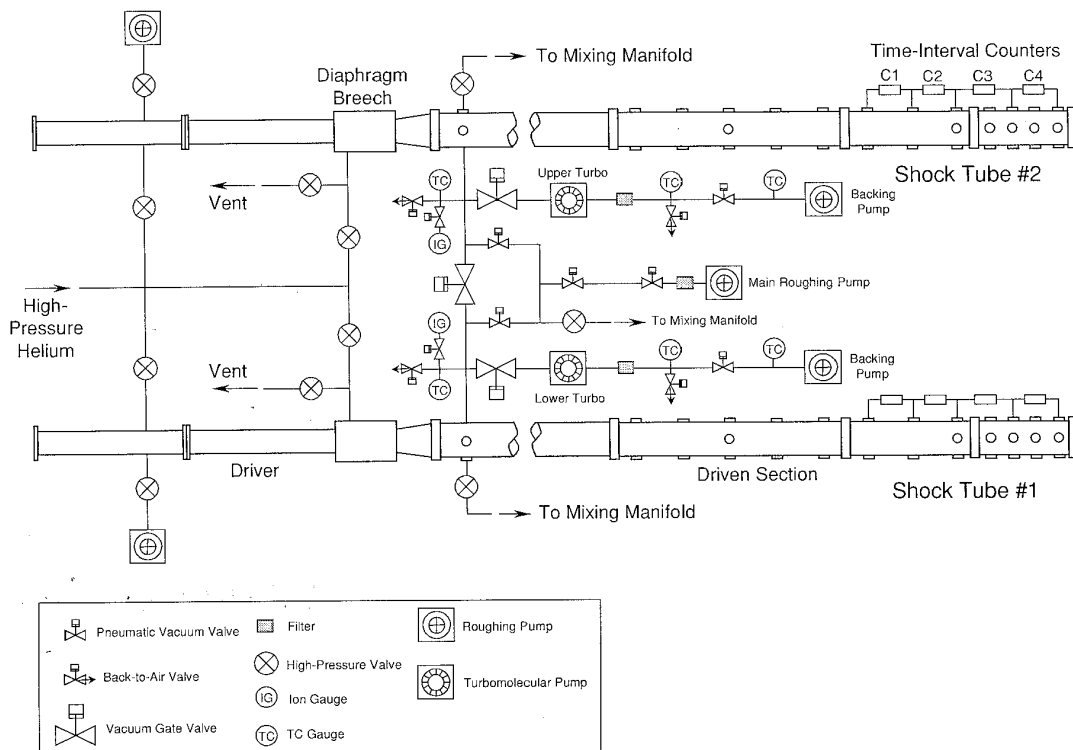


Figure 17: Schematic of the shock-tube facility used for the experiments. Only the lower shock tube was used herein [14].

Note that there are two identical tubes that are vertically aligned. In this study, only the lower tube was used for the experiments. Under normal circumstances, the shock tube is pressure-driven using helium as the driver gas. However, as mentioned in Chapter 2, driver-gas tailoring was used to create longer test times. This is discussed in more detail in the next section. For high-pressure experiments, pre-scored aluminum diaphragms of thickness ranging from 2-10 mm are used. The driver section is 3.5 m long and has an internal diameter of 7.62 cm. The driven section is 10.7 m long with an internal diameter of 16.2 cm. The endwall flange can be removed

for cleaning purposes. Light emission from CH^* chemiluminescence was collected through two CaF_2 windows, one located in the endwall and one located at the sidewall location. A schematic of the light detection system for both the endwall and the sidewall can be found in Fig 18.

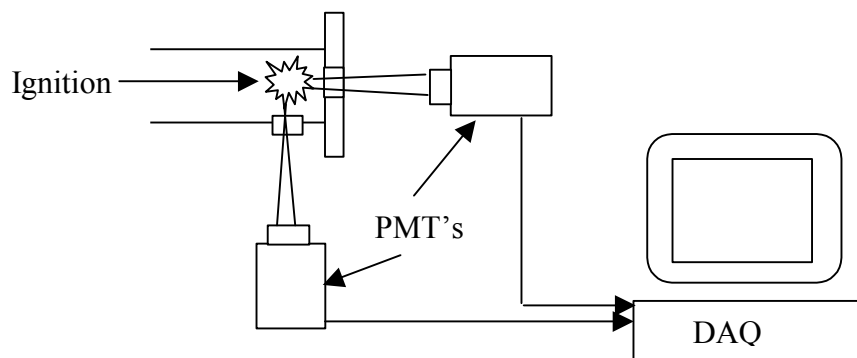


Figure 18: Schematic of the optical light detection system as employed in this study

Under low-pressure circumstances, three MKS baratron model PDR-C-1B pressure transducers with 0-10, 0-100, and 0-1000 Torr pressure ranges are used to measure the driven-section fill pressure (P_1). However, the fill pressures needed for high-pressure, low-temperature experiments, i.e., 1000-1200 Torr, fall outside the range of these pressure transducers. Therefore, a fourth pressure transducer is used with a range of 0-100 psi. Post-shock pressures cannot be measured using conventional, diaphragm-based pressure transducers. Therefore, a Kistler 603B1 piezoelectric pressure transducer in combination with a 5010 amplifier/signal conditioner box is used. This Kistler pressure transducer is located at the bottom of the tube, 1.6 cm from the endwall. This transducer is used to determine the qualitative, transient pressure and to ascertain the timing of the experiment. Absolute pressure readings are not obtained from this Kistler pressure transducer but instead are calculated using the shock speed in conjunction with the 1-D shock relations and the species thermodynamics.

The computer-based data acquisition consists of a desktop computer and two oscilloscope boards from Gage Applied Sciences. Four channels are available with a 12-bit resolution and a sampling rate of 5 MHz.

The vacuum system uses a Leybold TMP1000C turbomolecular pump (1000 l min^{-1}). A Leybold D16B (450 l min^{-1}) roughing pump backs up the turbomolecular pump. Initial roughing is done using a Kinney roughing pump. The vacuum system allows for evacuation to pressures below 10^{-6} torr. Note that in this specific study, the need for ultra- low vacuums is reduced by the fact that high-pressure gases are used to fill the tube to its initial condition, so the relative impurities are smaller. This allowed for faster ‘turn-around’ times in between experimental runs.

In most experiments, it is necessary that the shock velocity be known as accurately as possible. This is because the wave speed, in addition to the familiar gas dynamic equations for normal shocks, is used to obtain the temperature. In fact, the conditions behind the reflected shock wave depend only on the speed of the incident wave, the initial fill pressure conditions, and the known gas properties. The normal shock assumption is specifically valid ‘far’ away from the diagram. Non-ideal effects such as viscosity, imperfect diagram rupture and shock acceleration due to energy release in the reacting mixture can contribute to an axially non-uniform shock speed. To compensate for this natural attenuation of the shock, 5 individual piezo-electric pressure transducers (PCB P113A), with a time response less than $1 \mu\text{s}$ were used for the velocity measurements, providing 4 axial (and hence time) intervals. Each transducer circuit includes a charge-to-voltage amplifier (PCB 402M148) connected to the sensor by a 1-m low-noise, coaxial cable (PCB 003C03). Two PCB 482A18 exciter/output boxes accomplished the signal conditioning. Four Fluke PM6666/016 counters were used to measure the time intervals

between the pressure rise of the passing incident wave. A schematic of the velocity measuring setup can be seen in Fig. 19.

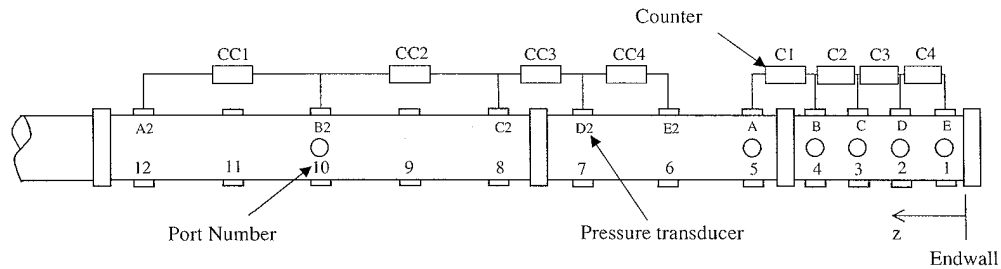


Figure 19: velocity detection system. In this study only the last four velocity measurements were used [14].

Note that only the last 4 counters (C_1 - C_4) were used for the velocity measurements. The additional counters that can be seen in Fig 19 were used by Petersen et al. [14] to investigate the attenuation of the velocity through the whole shock tube.

4.2 Mixtures

Twenty-one different mixtures were tested. These mixtures approach the mixtures that were initially set by Table 4 in Chapter 3. The mixture table with the mixtures created and used in this study can be found in Table 6. The right column shows the original mixture numbers from the L-21. Note that it was usually possible to reproduce the mixtures of the experimental design matrix within an accuracy of $< 1\%$ for each mole fraction. The gases used were ultra high purity (UHP) argon (99.995%), UHP O_2 , and research grade H_2 , CH_4 , C_2H_6 , C_3H_8 , C_4H_{10} , and C_5H_{12} . Partial pressure laws were used to create the mixtures. The fuel blends were mixed in a test-gas mixing tank through injection with a stinger tube containing hundreds of small outlet holes. This ensured homogenous mixtures. The vapor pressure of pentane is lower than atmospheric (± 0.5

atm at 293 K). Therefore, the pentane was allowed to vaporize into the evacuated mixing tank, after which the other fuel additives were added finishing with oxygen and argon.

Table 6: Experimental mixture table. The mixture numbers from the L21 can be found in the right column.

| L21 | T | CH4 | C2H6 | C3H8 | C4H10 | C5H12 | H2 |
|------------|----------|------------|-------------|-------------|--------------|--------------|-----------|
| 1 | 849 | 1.000 | 0 | 0 | 0 | 0 | 0 |
| 1 | 1107 | 1.000 | 0 | 0 | 0 | 0 | 0 |
| 2 | 811 | 0.750 | 0.250 | 0 | 0 | 0 | 0 |
| 3 | 817 | 0.751 | 0 | 0.249 | 0 | 0 | 0 |
| 3 | 1100 | 0.751 | 0 | 0.249 | 0 | 0 | 0 |
| 4 | 881 | 0.750 | 0 | 0 | 0.250 | 0 | 0 |
| 4 | 976 | 0.750 | 0 | 0 | 0.250 | 0 | 0 |
| 5 | 876 | 0.750 | 0 | 0 | 0 | 0.250 | 0 |
| 5 | 925 | 0.750 | 0 | 0 | 0 | 0.250 | 0.000 |
| 6 | 816 | 0.750 | 0 | 0 | 0 | 0 | 0.250 |
| 7 | 827 | 0.500 | 0.500 | 0 | 0 | 0 | 0 |
| 8 | 815 | 0.500 | 0.250 | 0.250 | 0 | 0 | 0 |
| 9 | 792 | 0.493 | 0.257 | 0 | 0.250 | 0 | 0 |
| 10 | 794 | 0.497 | 0.255 | 0 | 0 | 0.248 | 0 |
| 11 | 802 | 0.500 | 0.251 | 0 | 0 | 0 | 0.249 |
| 13 | 797 | 0.498 | 0.000 | 0.251 | 0.251 | 0 | 0 |
| 14 | 791 | 0.497 | 0 | 0.256 | 0 | 0.248 | 0 |
| 15 | 786 | 0.489 | 0 | 0.252 | 0 | 0 | 0.259 |
| 16 | 914 | 0.500 | 0 | 0 | 0.500 | 0 | 0 |
| 17 | 807 | 0.500 | 0 | 0 | 0.251 | 0.250 | 0 |
| 18 | 797 | 0.501 | 0 | 0 | 0.245 | 0 | 0.254 |
| 19 | 934 | 0.500 | 0 | 0 | 0 | 0.500 | 0 |
| 19 | 803 | 0.500 | 0 | 0 | 0 | 0.500 | 0 |
| 20 | 798 | 0.505 | 0 | 0 | 0 | 0.248 | 0.248 |
| 21 | 803 | 0.503 | 0 | 0 | 0 | 0 | 0.497 |

4.3 Uncertainty analysis

To do an uncertainty analysis, one should first see which parameter one is interested in and secondly on which quantities this parameter depends. Ideally there is a known functional relationship between one and the others. In the case of the present experiments, the main parameter of interest is the post-reflected-shock temperature, usually referred to as T_5 . If one

assumes constant specific heat ratio and the fact that the one-dimensional shock relations are valid, the reflected-shock temperature is a function of initial temperature (T_1), the gas specific heat ratio (γ), and the incident-shock Mach number (M) [40-43].

$$T_5 = \frac{T_1 [2(\gamma - 1)M^2 + (3 - \gamma)] [(3\gamma - 1)M^2 - 2(\gamma - 1)]}{(\gamma + 1)^2 M^2} \quad 1$$

In the case of the experiments herein, it can be shown that the specific heat ratio for a typical gas mixture ($\text{CH}_4/\text{O}_2/\text{Ar}$) with an equivalence ratio of $\phi = 0.5$ is ($\gamma = 1.61$). Equation 1 can then be reduced to an explicit correlation for T_5 (M):

$$T_5 = T_1 (0.686 M^2 + 0.563 - 0.249 M^2) \quad (2)$$

Note that the Mach number (M) is itself a function of γ , T_1 and the velocity shock-wave velocity V_w given by the functional relationship

$$M = \frac{V_w}{\sqrt{\gamma T_1 R}} \quad (3)$$

The accuracy of the temperature T_1 depends on the instrument resolution (1 °C), the accuracy of the thermocouple used, and the difference due to the spatial distribution. As said in 4.1, the velocity is inferred from 5 pressure transducers and 4 timers. The velocity at the endwall is determined by extrapolating a linear fit through the 4 velocity measurements. An example of this can be seen in Fig. 20. Note that there appears to be some random scatter around the linear

fit. The exact reason for this is not yet known [14] but is probably due to non-ideal shock formation/propagation effects or vibration that perturbs the trigger signal(s). The fact that a linear fit through this data is still better than using a single velocity measurement at the endwall was proven by Petersen et al. [14]. In the work by Petersen et al. [14] it was shown that the correlation through the four velocity measurements agrees well with linear fits through 9 velocity measurements over a much larger section of the tube (as in Fig. 19). Therefore, it is the author's belief that the standard error of estimate from the four-point correlation is better than that shown in Fig. 20 and is set to be 0.5 m/s in Table 5.

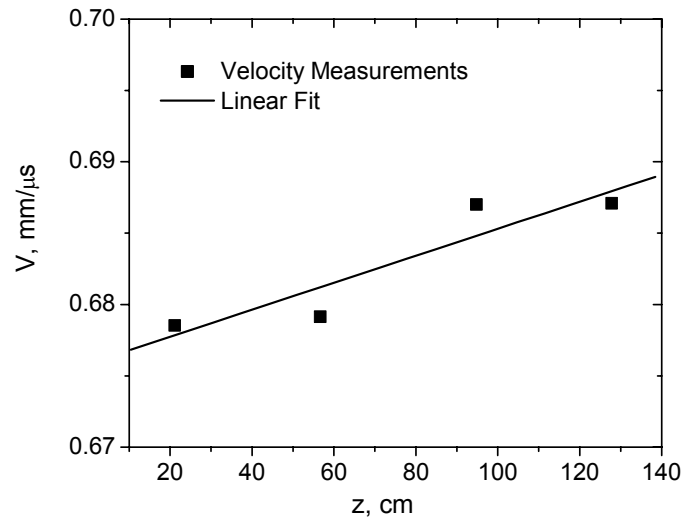


Figure 20: Linear fit through the four velocity measurements. Note that the distance z is the distance from the endwall and one is interested in the wave velocity at $z = 0$.

Next to the random error that comes from the linear fit through the four velocity measurements, there are two systematic errors, one for the distance measurement between ports and one for the time measurements from the timers. The random error caused by the linear fit is quantified by

the standard error of fit multiplied by the student t-factor. The number of degrees of freedom is 2, since there are four data point and 2 constants from the linear fit. A schematic of the shock-velocity measurement setup is given in Fig. 19. An organized presentation of the different elemental errors, both random and systematic, can be found in Table 7.

Table 7: Systematic and random uncertainties for the temperature (T_5) measurement.

| | Systematic | Random |
|-------------------------------------|-------------------|---------------|
| Velocity V_w | | |
| Distance (cm) | 0.013 | |
| Time (μs) | 0.665 | |
| Interpolation (mm/ μs) | | 0.0005 |
| Temperature T_1 | | |
| Intrumentation, C | 0.5 | |
| Accuracy, C | 0.5 | |
| Spatial, C | 1 | |

The uncertainty is then given by.

$$B_{T_1} = \sqrt{\sum_1^k \left(\frac{\partial T_5}{\partial V_w} w_{v_w} \right)^2 + \sum_1^k \left(\frac{\partial T_5}{\partial T_1} w_{T_1} \right)^2} \quad (4)$$

For the systematic error and

$$S_{T_1} = t_{95,2} \frac{\partial T_5}{\partial V_w} S_{V_w} \quad (5)$$

Note that the uncertainty is given with an accuracy of 95%.

The temperature T_5 with respect to the velocity V_w has a higher sensitivity at the conditions set for these experiments than the derivative with respect to temperature T_1 . It is therefore important that the velocity measurement be done as accurately as possible. This justifies the extra effort of using four velocity measurements together with a linear fit as opposed to a single velocity measurement. During shock-tube experiments, one should always keep the velocity sensitivity in mind. The resulting uncertainty is ± 8 K for experiments conducted at 800 K.

4.4 Shock-tube tailoring

To study combustion chemistry at low-to-intermediate temperatures, it is of great importance to increase the shock-tube test times. This can be done by tailoring the interface between the driver and driven gases. Shock tubes are commonly employed to study chemical kinetics and other combustion phenomena at elevated temperatures. Usually, shock-tube test times are on the order of 1 ms.

In a typical shock tube, the driven section is 3 times as long as the driver section, and the driver gas is usually helium. Helium, because of its low molecular weight, is a very efficient driver gas creating the highest pressure and temperatures with the lowest pressure differential across the diaphragm. A disadvantage of helium is its high sound speed. Large sound speeds lead to fast-propagating expansion waves, which ultimately end the test times. One way of decreasing the sound speed of the driver gas is to mix the helium with a heavier gas with the acceptance of the reduction in shock efficiency. The gas of choice for weighing down the driver gas depends on the geometry of the shock tube [44, 45]. The gas used for tailoring the shock tube depends

next to its molecular weight on the specific heat ratio. The tailoring section included in this thesis describes the tailoring method as developed by Amadio et al. [44, 45], and is employed in this study in order to create longer test times.

The shock-tube test time is defined as the time between the passing of the reflected shock wave and the arrival of the next wave, usually the expansion wave coming from the driver section. As said, strong incident shock waves are desired for high test temperatures (T_5), therefore helium is usually the gas of choice for the driver gas. Figure 21 shows an x-t diagram that explains what happens in a ‘tailored’ case.

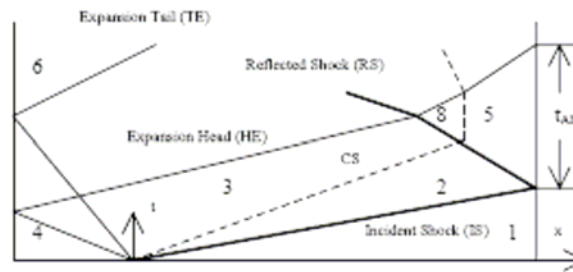


Figure 21: x-t diagram for ‘tailored’ case. The contact surface remains stationary when $P_8 = P_5$. From Amadio et al. [44].

Tailored in this thesis means that there is no pressure discontinuity at point ‘p’ where the reflected shock collides with the contact surface, $P_8 = P_5$. As a result, the contact surface appears stationary, and the test section becomes more or less isolated from wave interaction outside the experimental region until the delayed expansion head reaches the test location (Fig. 21).

After the rupture of the diaphragm, a series of expansion waves will move toward the end of the driver section, traveling at the local speed of sound (1016 m/s for helium). When they reach the endwall of the driver section, they will bounce back and move in the opposite direction at a lower velocity. Due to superposition of the bulk motion of the gas on top of the speed of the

expansion wave, the expansion wave will accelerate to velocities greater than their original velocities relative to the shock-tube fixed reference frame. For test temperature T_5 between 700 and 1400 K, the contact surface between the driver gas and driven gas travels at a velocity of 240-470 m/s in Argon. The gas-dynamic behavior within a shock tube depends both on the thermodynamic properties of the gases as well as the shock-tube geometry. Fortunately, the experiments herein were performed ideally under the same operational conditions. Therefore, it was only necessary to find one ideal driver gas composition that would allow for the longest test time. In general, there is a tailored composition for each temperature, making true tailored conditions hard to achieve in practice.

Since the expansion waves travel at the local speed of sound of the gas they occupy, their speeds can be greatly reduced by reducing the speed of sound of the gas. The sound speed is a function of the gas constant, the specific heat ratio, and the temperature. Lowering the temperature of the driver gas is usually not a feasible option. Therefore a heavier gas must be used to lower the sound speed. This would postpone the arrival of the expansion wave at the shock-tube end wall. Amadio et al. developed a 1-D gas dynamic model of the shock tube. The assumptions were adiabatic flow, non-reacting, 1-D flow, perfect gas and no molecular diffusion.

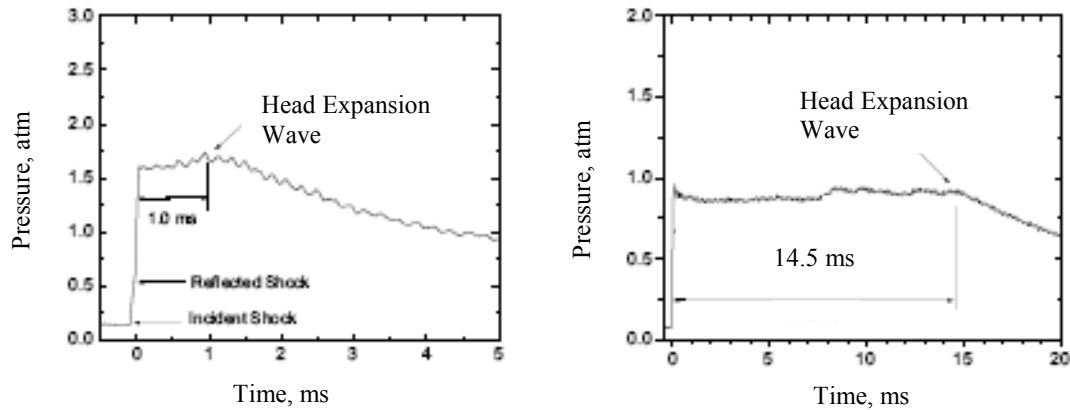


Figure 22: Pressure trace for untailed and tailored conditions respectively. Note that test times of 14+ ms can be obtained by using a heavier driver gas. This case, He/CO₂ 70/30%

To create a reflected-shock test pressure of 22 atm, the driver-gas pressure P_4 needed to be around 1400 psi. Therefore, a tailor gas was chosen that would remain a gas at high pressures, i.e. the vapor pressure needed to be high. For this reason, CO₂ was chosen to accompany the helium in the driver section. The vapor pressure of CO₂ at 293 K is about 1000 psi. Note that this is less than P_4 , however, it was estimated by Amadio et al. that only 30-35 % CO₂ was needed to create tailored conditions, which results in partial pressures between 420 and 490 psi [44,45]. Figure 22 shows the pressure trace without and with shock-tube tailoring, respectively. It can be seen in Fig. 22 that it was possible to create test times on the order of 14 ms, as opposed to the 1-ms test times under untailed conditions. The pressure traces from the experimental runs as shown in appendix A have all used similar driver-gas tailoring to create these long test times.

4.5 Results

The intent of the experiments was to show the effect of higher-order hydrocarbons on the ignition behavior of methane base mixtures at 800 K and around 20 atm. Next to providing valuable data to those involved in combustor design, the data can be used to validate chemical kinetics mechanisms in this relatively unknown low-temperature, high-pressure regime.

Table 6 shows the mixtures that were created for the experiments. Next to mixtures that were produced to test the best tailoring mixtures, a total of 21 mixtures were created and used for the actual autoignition experiments. The initial driven pressure P_1 (1000-1100 Torr) required the gas of three separate mixing tanks out of a total of four. Since the initial fill pressure sets the temperature given a certain diaphragm thickness, the remainder of the mixture was sometimes used to create an extra run at higher temperature. Although this higher temperature falls outside the region of interest herein, it still provides valuable information in terms of temperature dependency.

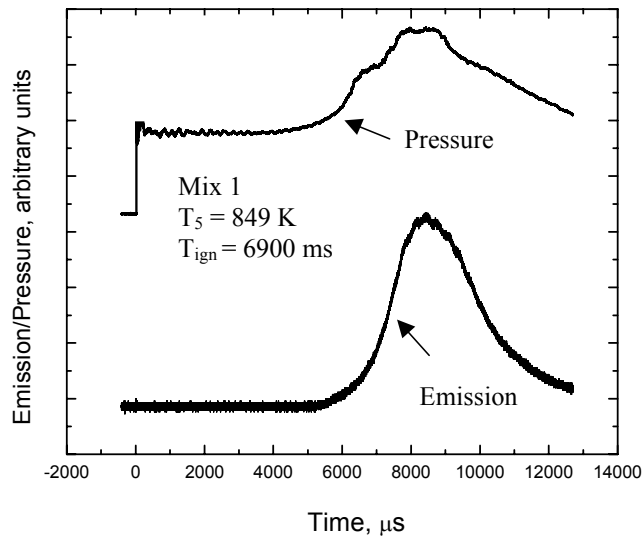


Figure 23: Pressure and emission plot for a pure methane case (mix. 1) at 849 K. Note the gradual buildup of pressure and emission called ‘weak’ ignition.

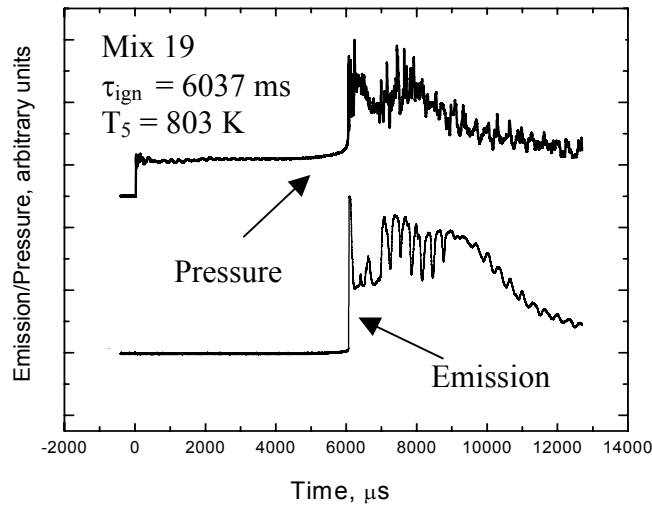


Figure 24: Pressure and emission trace from a methane and pentane mixture (mix. 19). The steep pressure and emission rise due to ignition is called ‘strong’ ignition.

(For this reason the temperature is included in the final correlation as an independent variable, as described below.) Figure 23 shows an experimental run with a pure methane mixture. Note the

gradual buildup of pressure and emission. This can be compared against Fig. 24, which is a mixture of CH₄ and C₅H₁₂. Note the almost step increase in pressure and emission in this case, referred to in the literature as strong ignition. Thus, a preliminary look at the experimental data shows that there is not only a difference in ignition delay, a quantity of most interest herein, but that there is also a fundamental difference in ignition behavior as can be seen in Fig 23 and Fig. 24. The pressure and emission traces of all other experimental runs can be found in Appendix A.

Table 8: Mixture table with experimental result in ms. The prediction by the chemical kinetics model at 800 K is also given. Note the large difference in experimental results and the model predictions Model was evaluated at 800 K.

| L21 | T | Model | | | | | | Exp | |
|-----|------|-------|-------|-------|-------|-------|-------|-------------|--------------|
| | | CH4 | C2H6 | C3H8 | C4H10 | C5H12 | H2 | tign (ms) | |
| 1 | 849 | 1.000 | 0 | 0 | 0 | 0 | 0 | 1710 | 7.00 |
| 1 | 1107 | 1.000 | 0 | 0 | 0 | 0 | 0 | | 2.35 |
| 2 | 811 | 0.750 | 0.250 | 0 | 0 | 0 | 0 | 1650 | 7.72 |
| 3 | 817 | 0.751 | 0 | 0.249 | 0 | 0 | 0 | 630 | 10.79 |
| 3 | 1100 | 0.751 | 0 | 0.249 | 0 | 0 | 0 | | 1.45 |
| 4 | 881 | 0.750 | 0 | 0 | 0.250 | 0 | 0 | 42 | 5.07 |
| 4 | 976 | 0.750 | 0 | 0 | 0.250 | 0 | 0 | | 4.24 |
| 5 | 876 | 0.750 | 0 | 0 | 0 | 0.250 | 0 | 24 | 5.42 |
| 5 | 925 | 0.750 | 0 | 0 | 0 | 0.250 | 0.000 | | 4.58 |
| 6 | 816 | 0.750 | 0 | 0 | 0 | 0 | 0.250 | 2310 | 8.10 |
| 7 | 827 | 0.500 | 0.500 | 0 | 0 | 0 | 0 | 1770 | 9.69 |
| 8 | 815 | 0.500 | 0.250 | - | - | - | - | 790 | 6.92 |
| 9 | 792 | 0.493 | 0.257 | - | - | - | - | 73 | 11.96 |
| 10 | 794 | 0.497 | 0.255 | 0 | 0 | 0.248 | 0 | 36 | 7.90 |
| 11 | 802 | 0.500 | 0.251 | 0 | 0 | 0 | 0.249 | 1820 | 7.80 |
| 13 | 797 | 0.498 | 0.000 | 0.251 | 0.251 | 0 | 0 | 71 | 9.32 |
| 14 | 791 | 0.497 | 0 | 0.256 | 0 | 0.248 | 0 | 37 | 8.36 |
| 15 | 786 | 0.489 | 0 | 0.252 | 0 | 0 | 0.259 | 64 | 8.58 |
| 16 | 914 | 0.500 | 0 | 0 | 0.500 | 0 | 0 | | 4.00 |
| 17 | 807 | 0.500 | 0 | 0 | 0.251 | 0.250 | 0 | 17 | 5.34 |
| 18 | 797 | 0.501 | 0 | 0 | 0.245 | 0 | 0.254 | 38 | 10.38 |
| 19 | 934 | 0.500 | 0 | 0 | 0 | 0.500 | 0 | | 3.69 |
| 19 | 803 | 0.500 | 0 | 0 | 0 | 0.500 | 0 | 13 | 6.04 |
| 20 | 798 | 0.505 | 0 | 0 | 0 | 0.248 | 0.248 | 21 | 5.98 |
| 21 | 803 | 0.503 | 0 | 0 | 0 | 0 | 0.497 | 2800 | 7.70 |

Table 8 shows all mixtures that were created plus the experimentally obtained ignition delay times. Note that the modeling result is at 800 K.. Note the significant difference between experimental result and the prediction by the model made earlier in most cases. This is particularly evident when higher-order hydrocarbons are not present. This is most likely due to the fact that the chemical kinetics model was calibrated against heptane and pentane mixtures at higher temperature and not with methane-based mixtures at lower temperatures, although it does contain higher-temperature methane chemistry as a subset. Hence, the Lawrence Livermore model shows poor agreement for pure methane or hydrogen mixtures at low temperature (< 1100 K) this was expected since it was calibrated for mixtures in this regime.

A correlation has been obtained to correlate the data in much the same way as has been done for the modeling data in Chapter 3. The correlation is given by:

$$\ln(\tau_{ign}) = 5.837 + \ln(3 - CH_4) + \ln(1 - C_2H_6) + \ln(1 - C_3H_8) + \ln(1 - C_4H_{10}) + \ln(1 - C_5H_{12}) + \ln(1 - H_2) + \frac{4646}{T}$$

(6)

And the parity plot that comes with the correlation can be seen in Fig. 25.

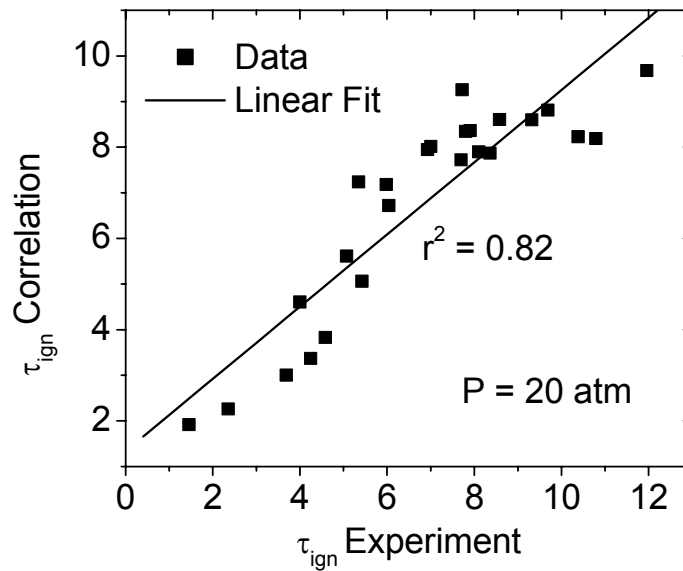


Figure 25: Parity plot for the experimental result against the correlation.

The correlation is in the typical Arrhenius form similar to that used in Chapter 3.

Table 9: Effect of amount of additive per species.

| Mix | τ_{ign} 75/25%, ms | τ_{ign} 50/50%, μs |
|---|--------------------------------|---|
| CH ₄ /C ₂ H ₆ | 7722 | 9691 |
| CH ₄ /C ₃ H ₈ | 10792 | -- |
| CH ₄ /C ₄ H ₁₀ | -- | -- |
| CH ₄ /C ₅ H ₁₂ | 5424 | 6037 |
| CH ₄ /H ₂ | 8100 | 7698 |

It would be interesting to see the effect of the amount of additive on the ignition behavior. Table 9 shows the difference between 75/25% and 50/50% mixtures. Note that the quantity of an additive does not seem to have a strong effect on the ignition delay time under these conditions.

Adding more C_2H_6 seems to slow the ignition down. This is the opposite of the ethane effect at higher temperatures [6].

The difference between strong versus weak ignition has already been seen in Fig. 23 and Fig. 24. This is an effect that is hard to quantify by a correlations since it is a Boolean (yes/no) phenomenon. There are only two mixtures that show ‘weak’ ignition behavior. These are the pure CH_4 mixture and the 75/25% CH_4/H_2 mixture. It is interesting that when more H_2 is added, there is a strong ignition as can be seen in Fig. 26 and Fig. 27.

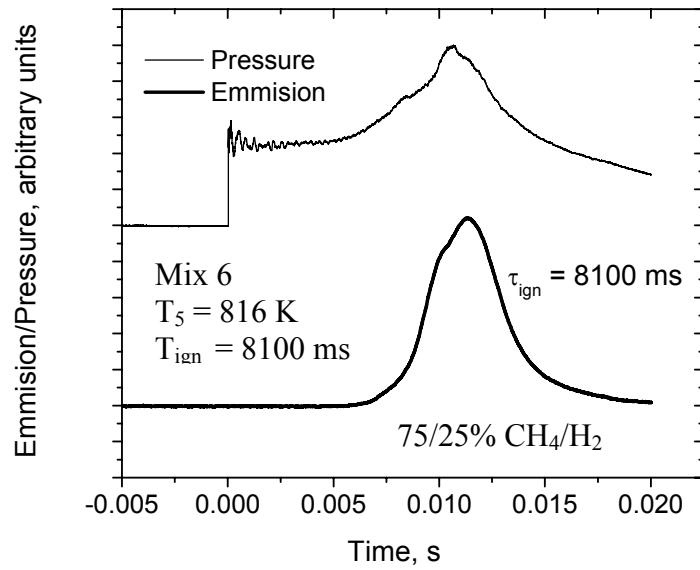


Figure 26: CH_4/H_2 75/25% Mixture (mix. 6) at 816 K. Note the weak ignition.

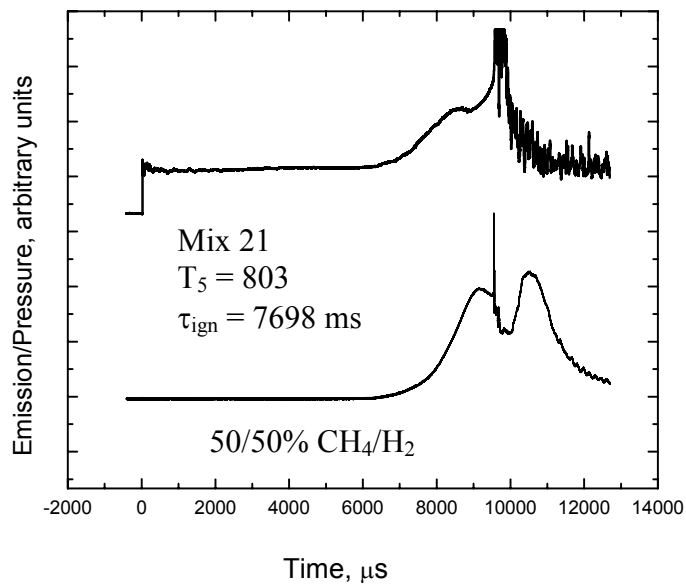


Figure 27: CH_4/H_2 50/50% Mixture (mix. 6) at 816 K. Note the strong ignition.

Since the values from the experiment are so close together, it makes sense to determine the sample mean of all the experiments around 800 K and see what the standard deviation will be. The sample mean of the experimental results from Table 7 is 7.90 ms with a standard deviation of 1.92 ms. This means that for any mixture of CH₄ with C₂H₆/C₃H₈/C₄H₁₀/C₅H₁₂/H₂ at 800 K and around 20 atm the ignition delay time will likely be 7.9 ± 3.84 ms, 95% of the time.

An interesting observation can be made when focusing on the pure methane blends, which are plotted in Fig. 28. It can be seen that the slope of the graph reduces when entering the low temperature regime. This indicates a reduction in activation energy. One very important observation is that the two new data points obtained in this study connected to previously obtained CH₄ data [36], seem to form one continuous graph. This would indicate that the low temperature data were shock tube tailoring is employed can seamlessly be connected to other and previously obtained high temperature data.

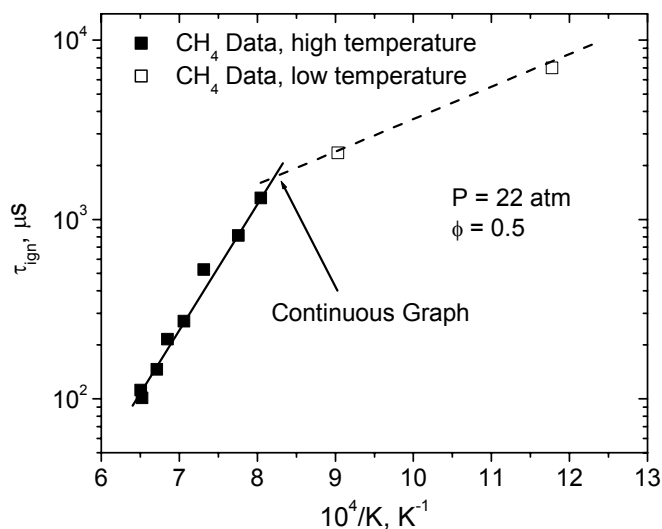


Figure 28: CH₄ Data from this study compared against CH₄ data previously obtained. Note the shift in activation energy and the way the data connects.

Figure 29 shows the pure methane together with all the experimental results from Table 8. Two 3rd order polynomials have been obtained to correlate the data for both pure CH₄ mixtures as well as for mixtures that include higher order hydrocarbons. Since the effect of hydrocarbon addition on CH₄ ignition was very similar, there was no attempt made to correlate the effect of each hydrocarbon addition individually.

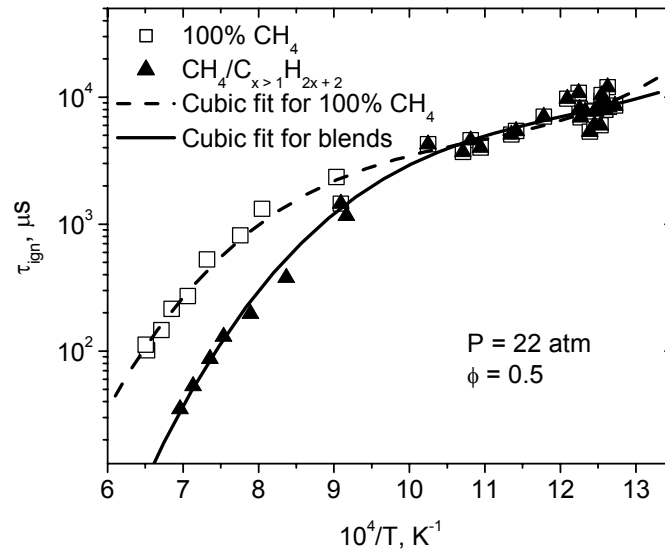


Figure 29: Data for pure CH₄ and mixtures both plotted against $10^4/T$. Two correlations are obtained for the two different cases.

Thus in the case of fuel lean ($\phi = 0.5$) combustion around 20 atm and at temperature between 1450-800 K, the ignition delay time can be predicted by using the following correlations.

$$\text{Log}(\tau_{ign})_{100\%CH_4} = -14.589 + 4.803 \left(\frac{10^4}{T} \right) - 0.432 \left(\frac{10^4}{T} \right)^2 + 0.01329 \left(\frac{10^4}{T} \right)^3 \quad (7)$$

$$\text{Log}(\tau_{ign}) = -19.267 + 5.464\left(\frac{10^4}{T}\right) - 0.440\left(\frac{10^4}{T}\right)^2 + 0.0121\left(\frac{10^4}{T}\right)^3 \quad (8)$$

These correlations give a r^2 value of 0.981 and 0.983 respectively.

CHAPTER 5: CONCLUSION AND RECOMMENDATIONS

5.1 Conclusions

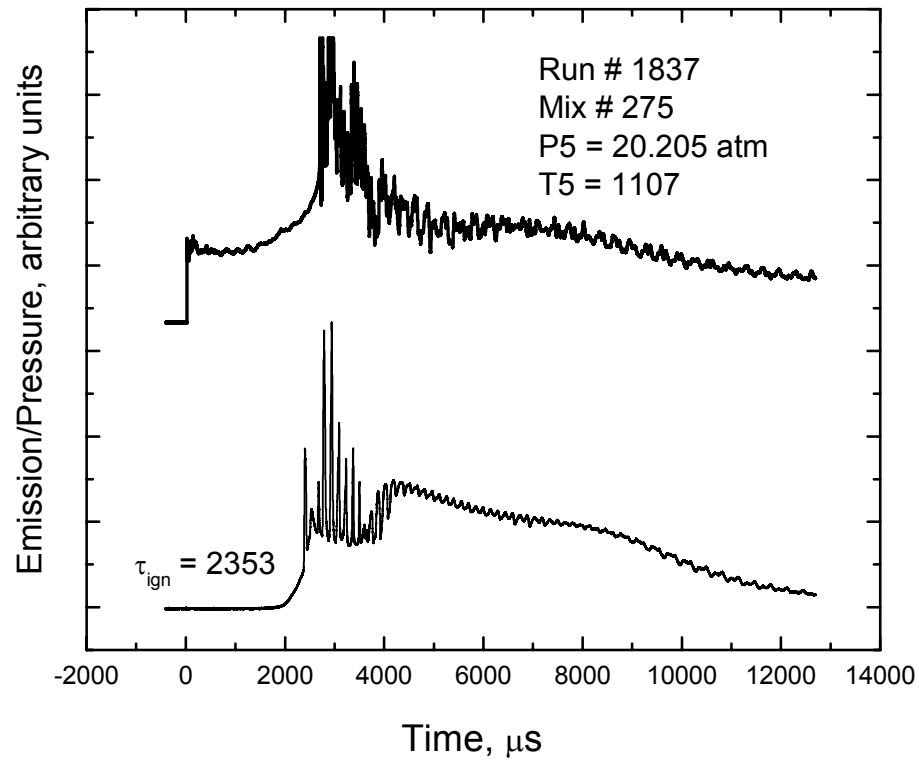
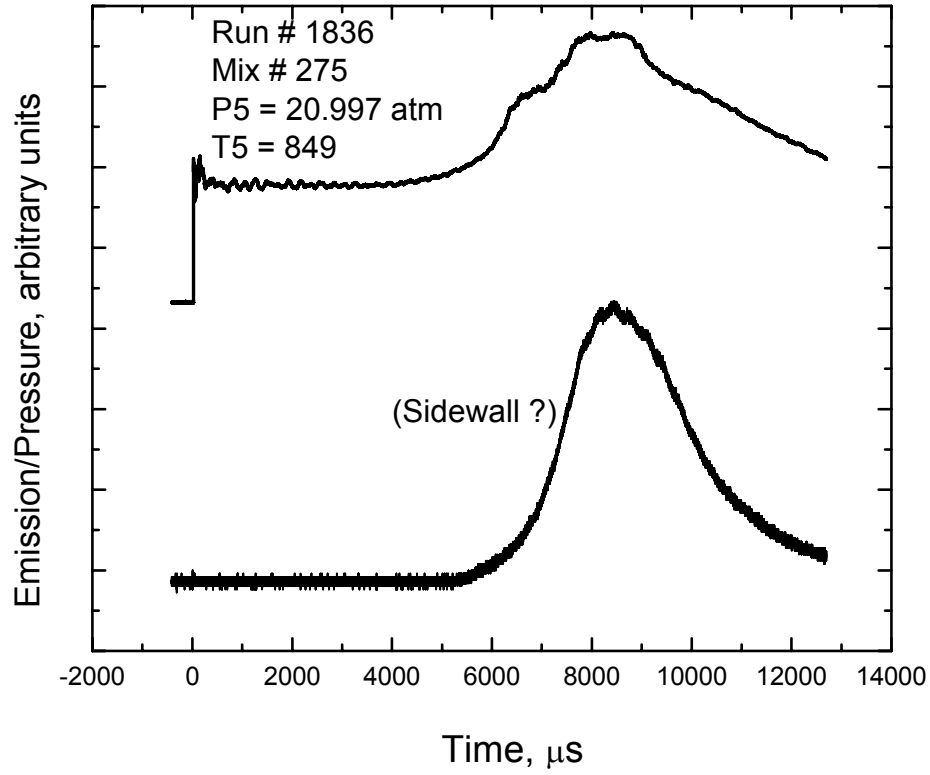
After carefully designing an experimental matrix, dictating that 21 different mixtures were necessary, 21 mixtures were created for experimental usage. After reviewing the chemical kinetic models predictions, it was the author's belief that the ignition delay time of many of the mixtures would fall outside the experimental range that could be obtained with the shock tube (10-14 ms), and would simply show no ignition at all. Fascinatingly, the experimental results show that all the mixtures ignited within the experimental time available, showing that methane-based mixtures are far more reactive at high pressures (20 atm) and low temperature (800 K) than previously thought. The variation in ignition time between the different mixtures was far less than expected. All the experimental results centered on a mean of 7.9 ms with a standard deviation of 1.92 ms. The danger of these mixtures igniting within the residence time of a power generation gas turbine is greater than previously thought. However, individual hydrocarbon additives do not seem to increase this threat.

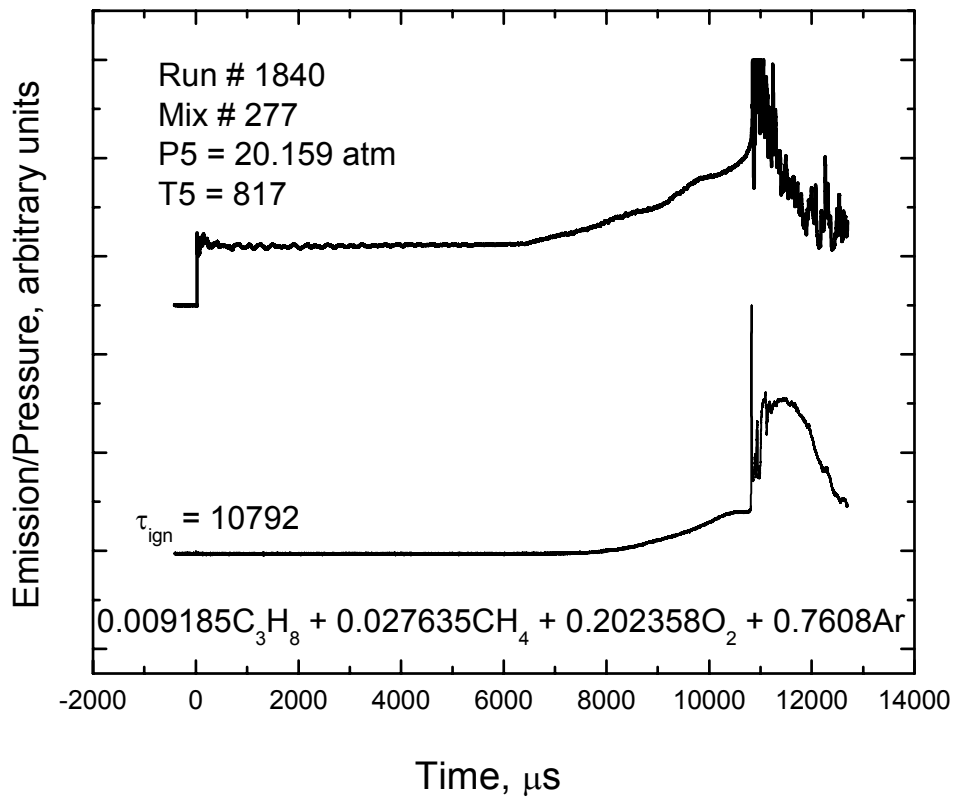
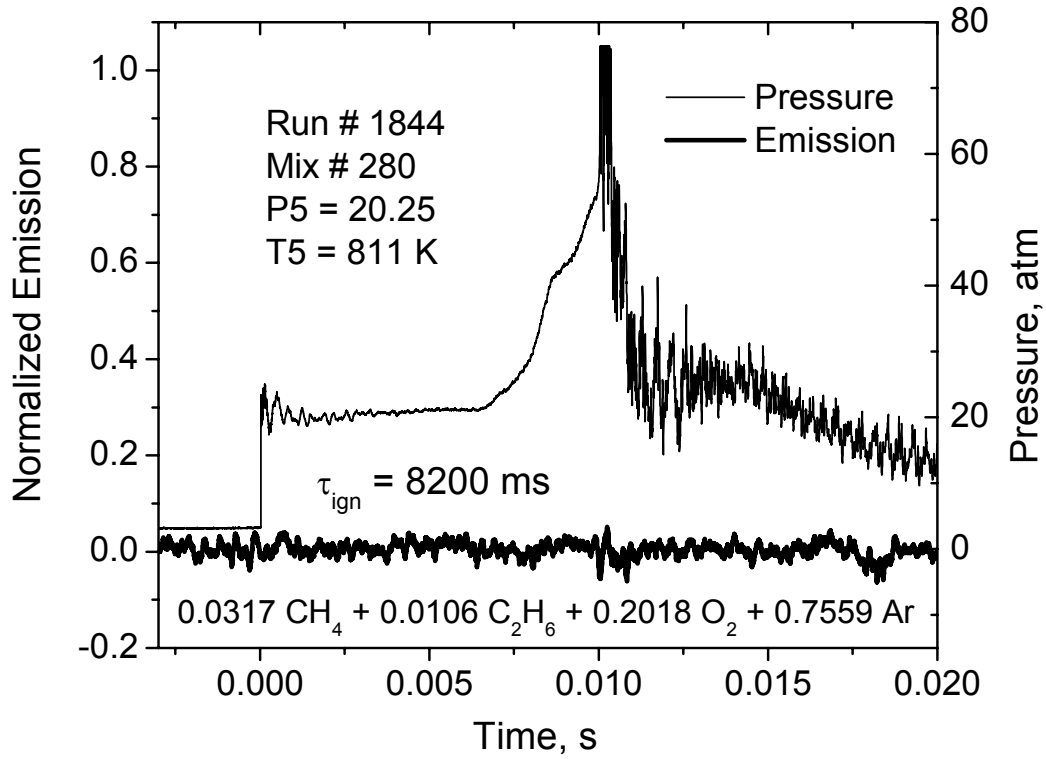
Besides the ignition delay time, higher-order hydrocarbons tend to have an effect on the ignition behavior of the fuel-blend mixture, showing 'weak' ignition for pure methane blends and 'strong ignition' for all other blends that include higher order hydrocarbons.

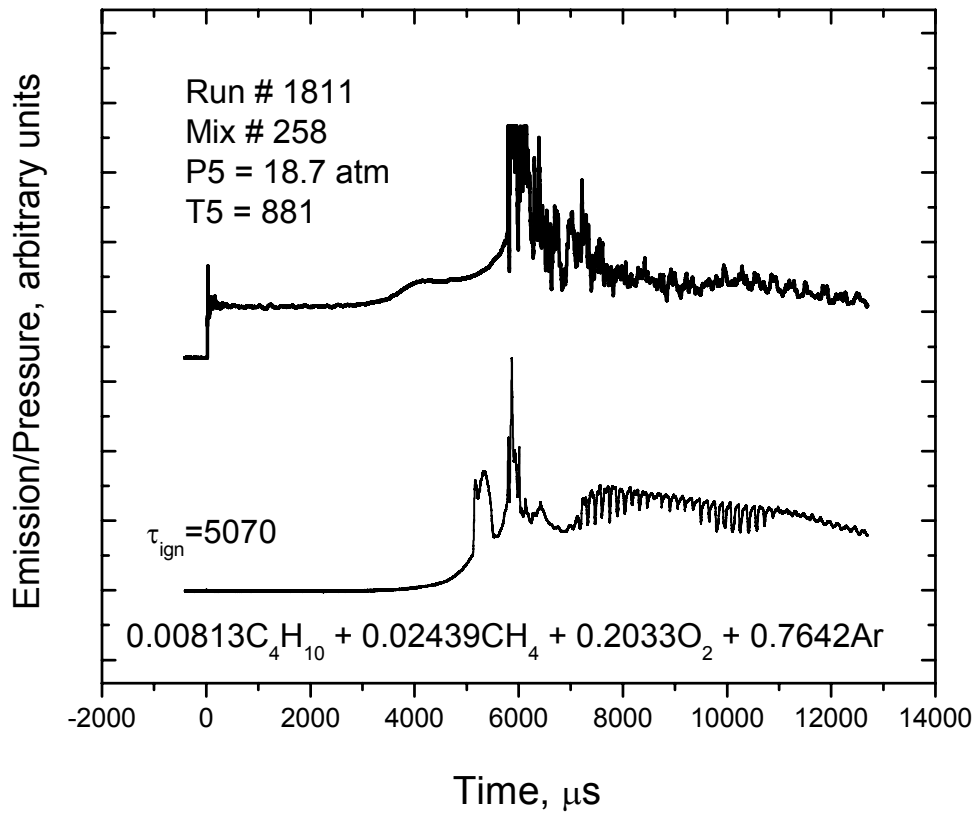
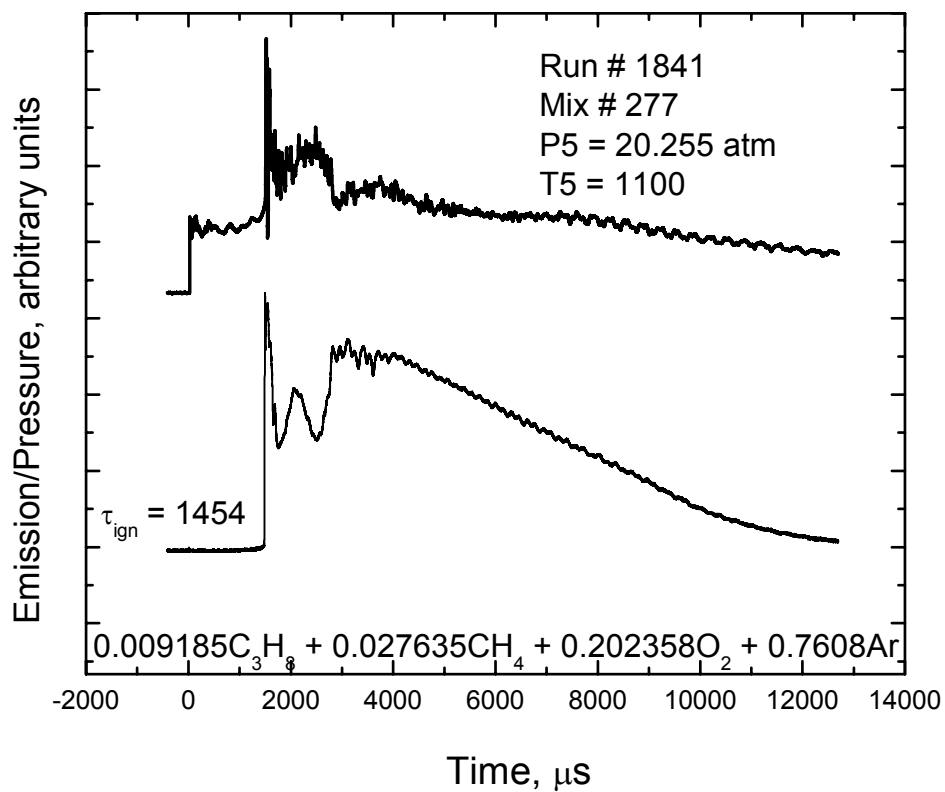
5.2 Recommendations

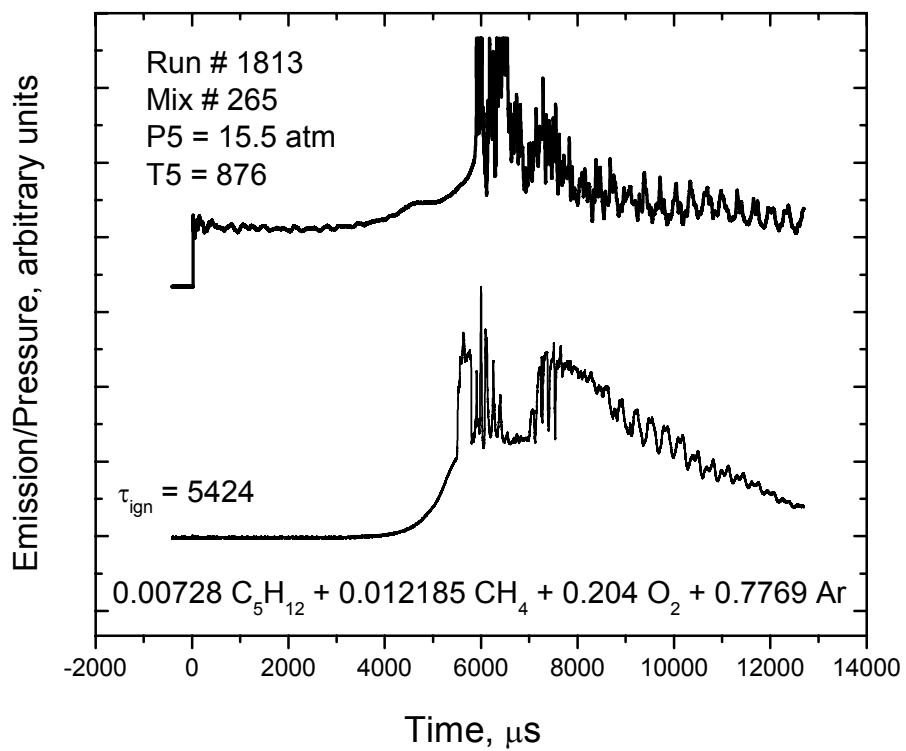
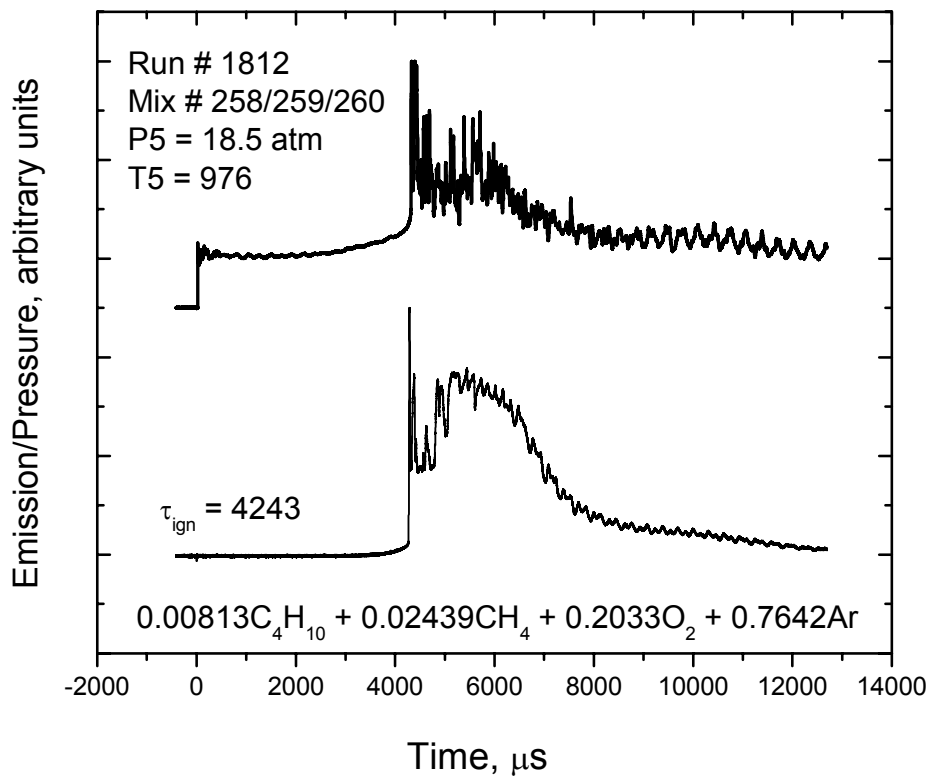
Since even pure methane blends at low temperatures and high pressure tend to be far more reactive than previously thought, it is recommended that a further investigation will be conducted in the methane ignition behavior at low-to-intermediate temperatures. Since the effect of significant amounts of higher-order hydrocarbon additives seems marginal, it would be interesting to investigate every individual hydrocarbon at low-to-intermediate temperatures. In this way, it can be determined if the similarity in ignition delay time between the different mixtures is caused by the dominating methane chemistry in this regime or that all hydrocarbons tend to show similar behavior at low temperature and high pressures.

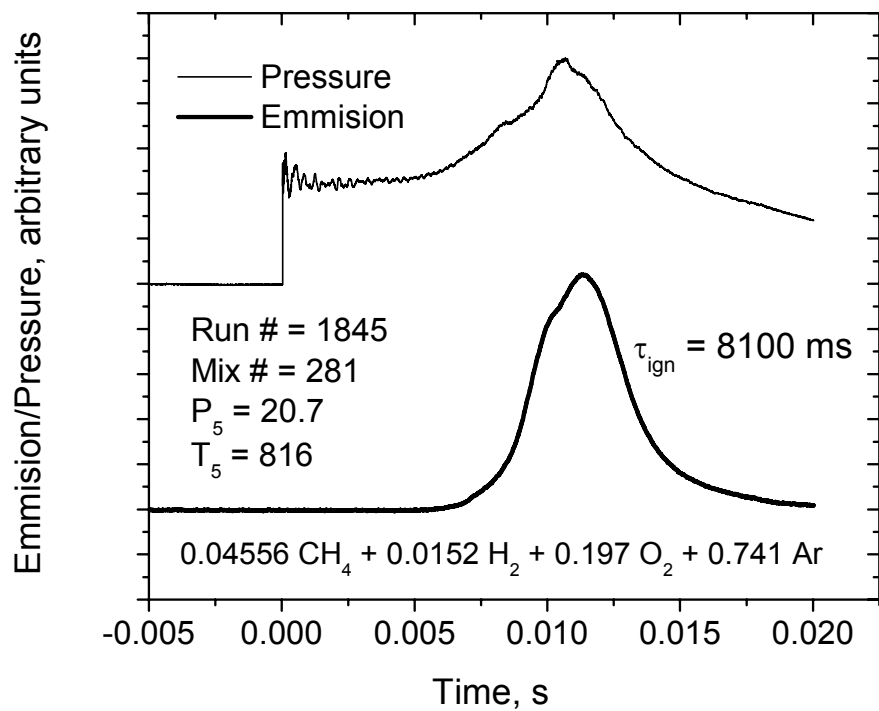
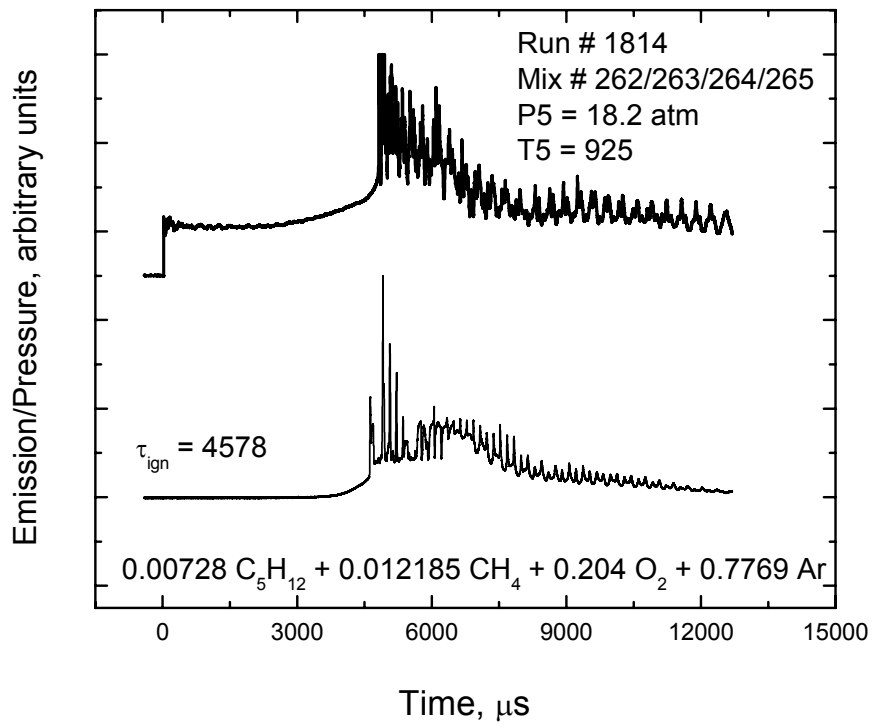
APPENDIX A: PRESSURE AND EMISSION PLOTS FROM EXPERIMENT

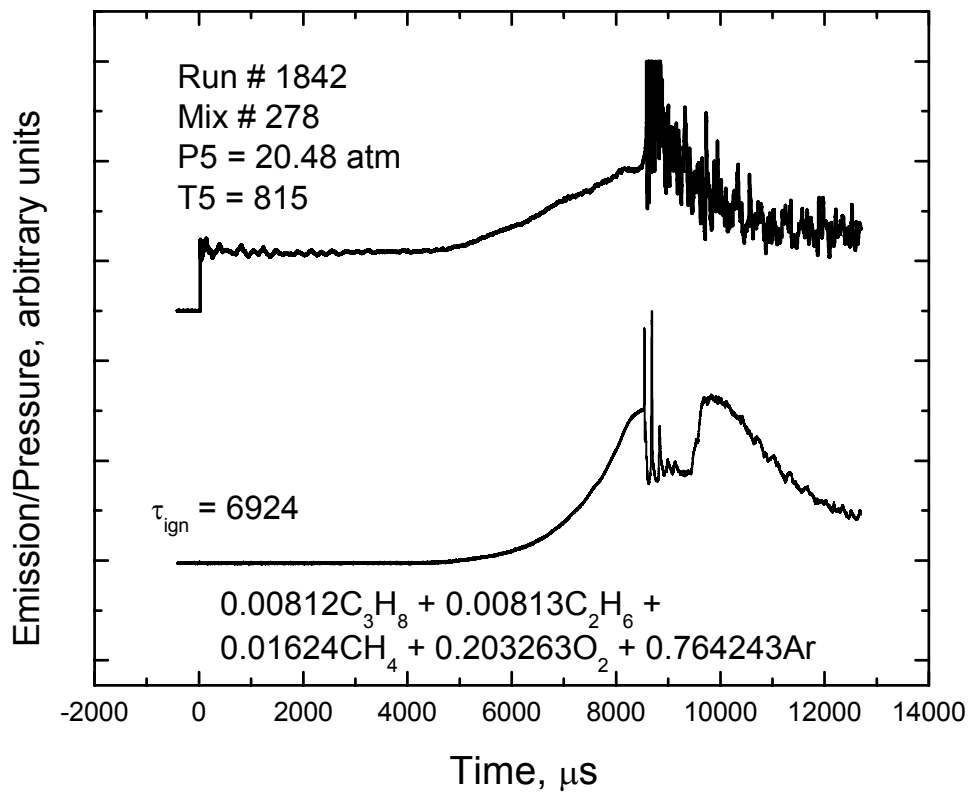
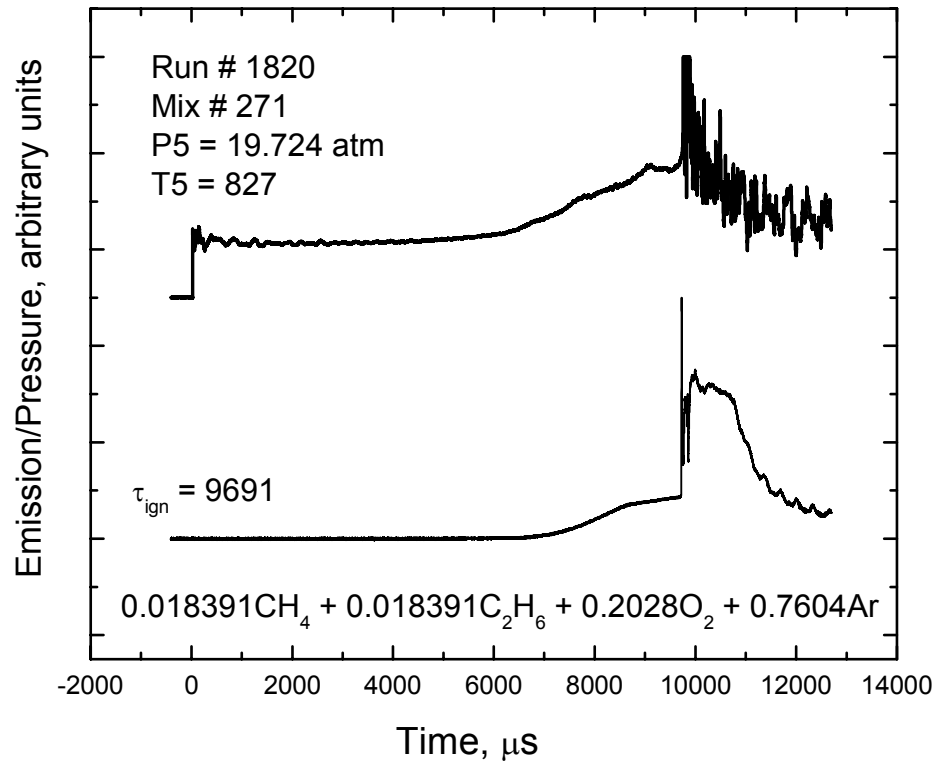


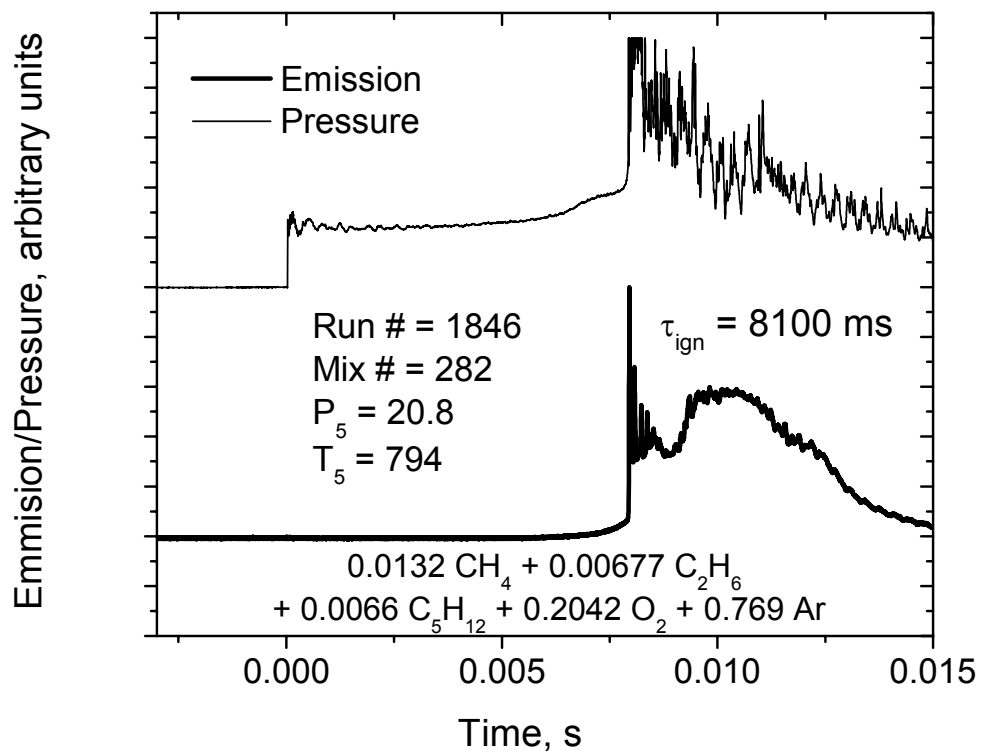
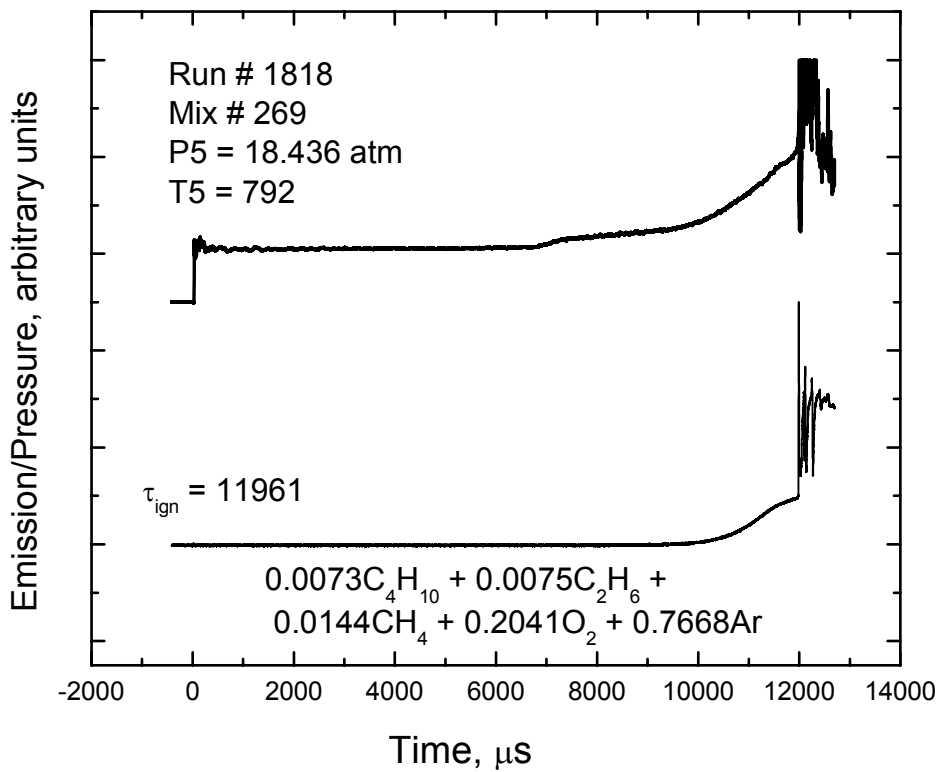


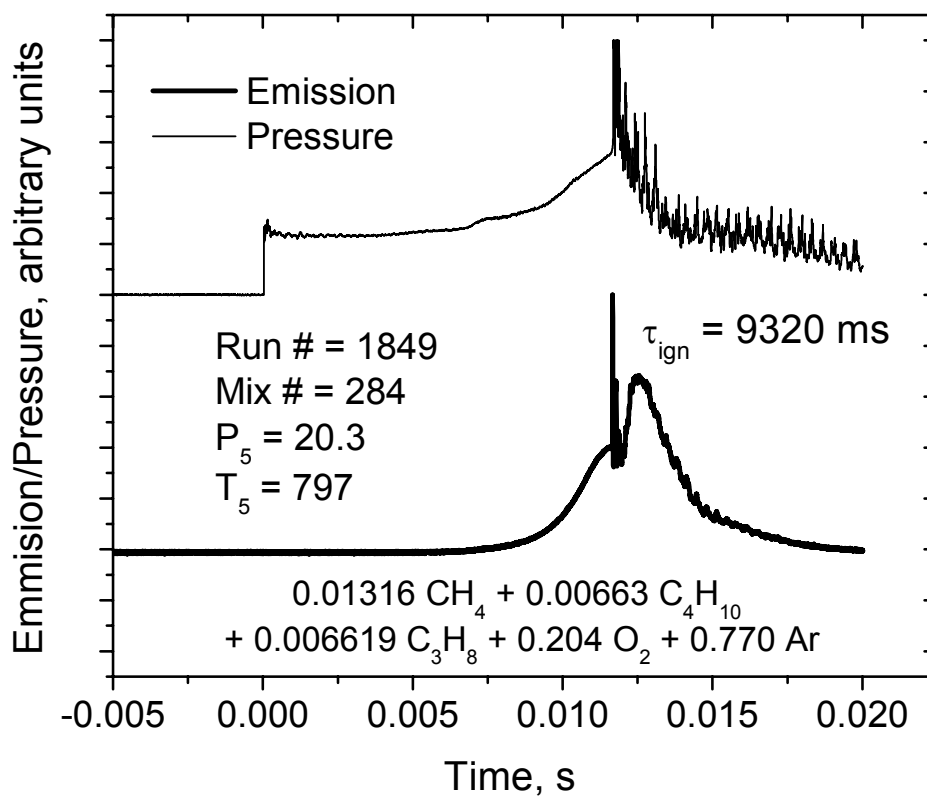
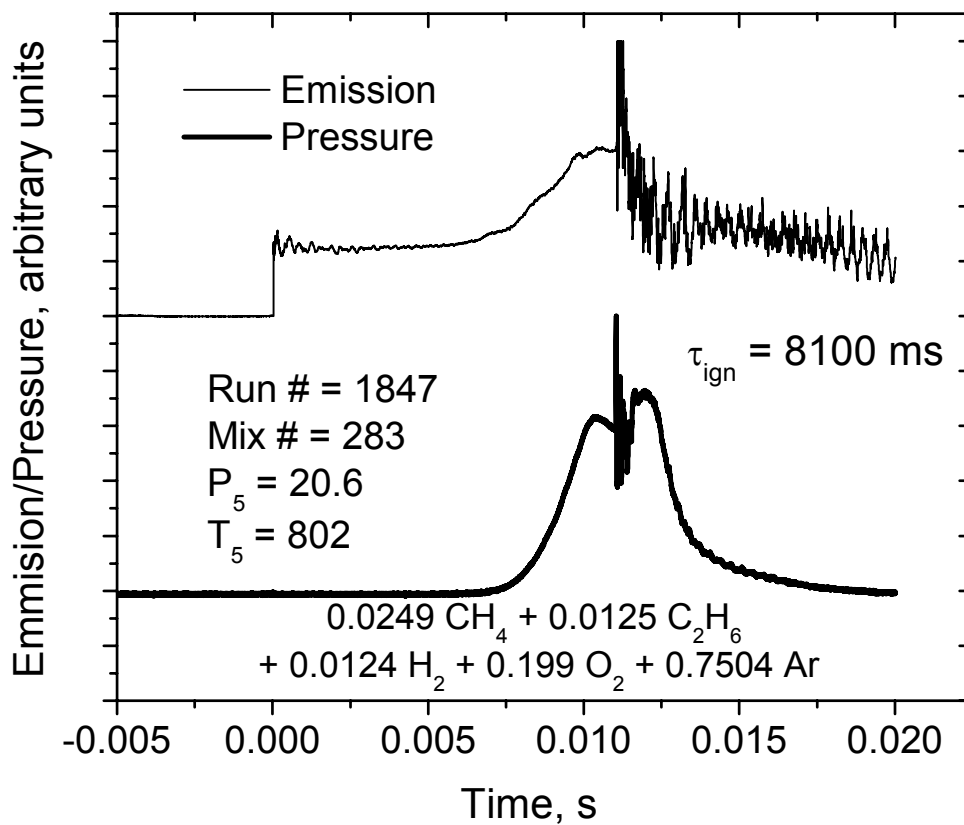


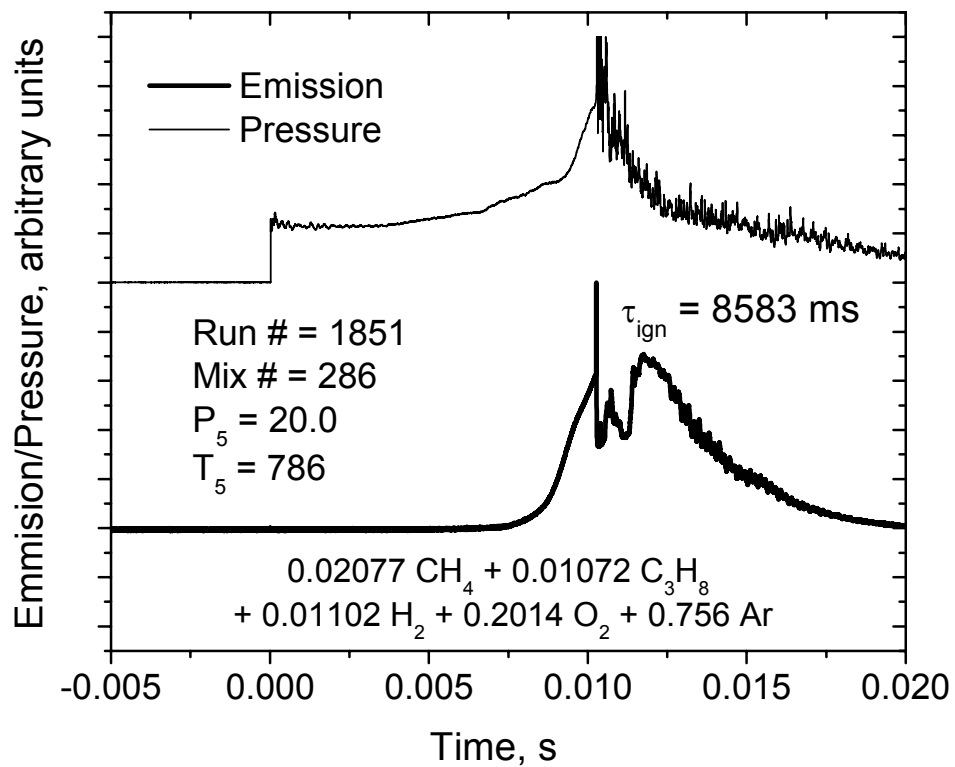
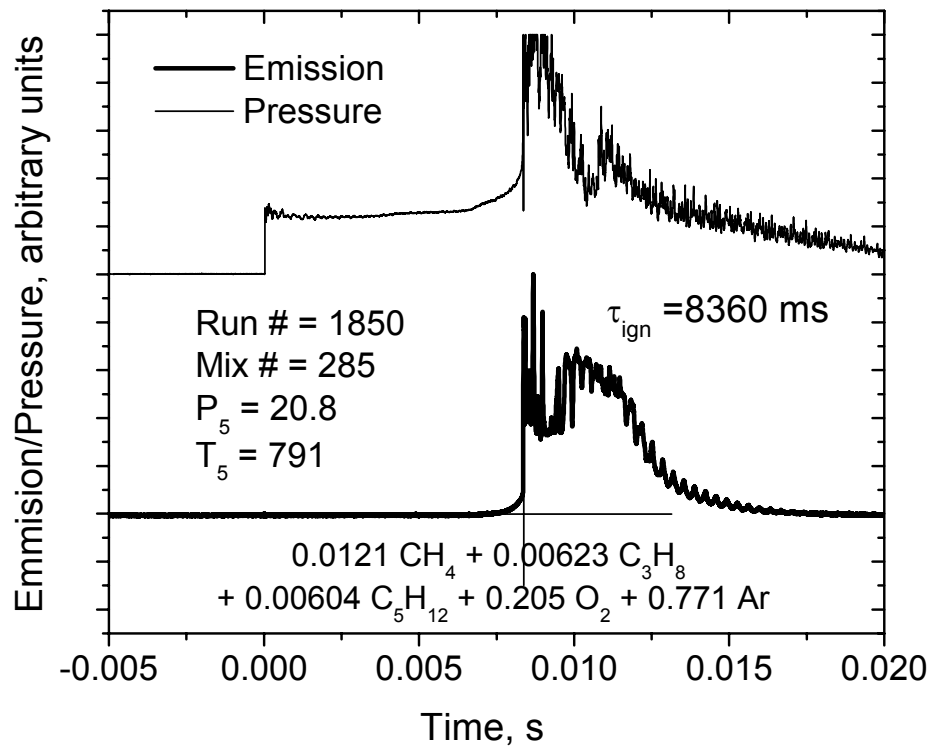


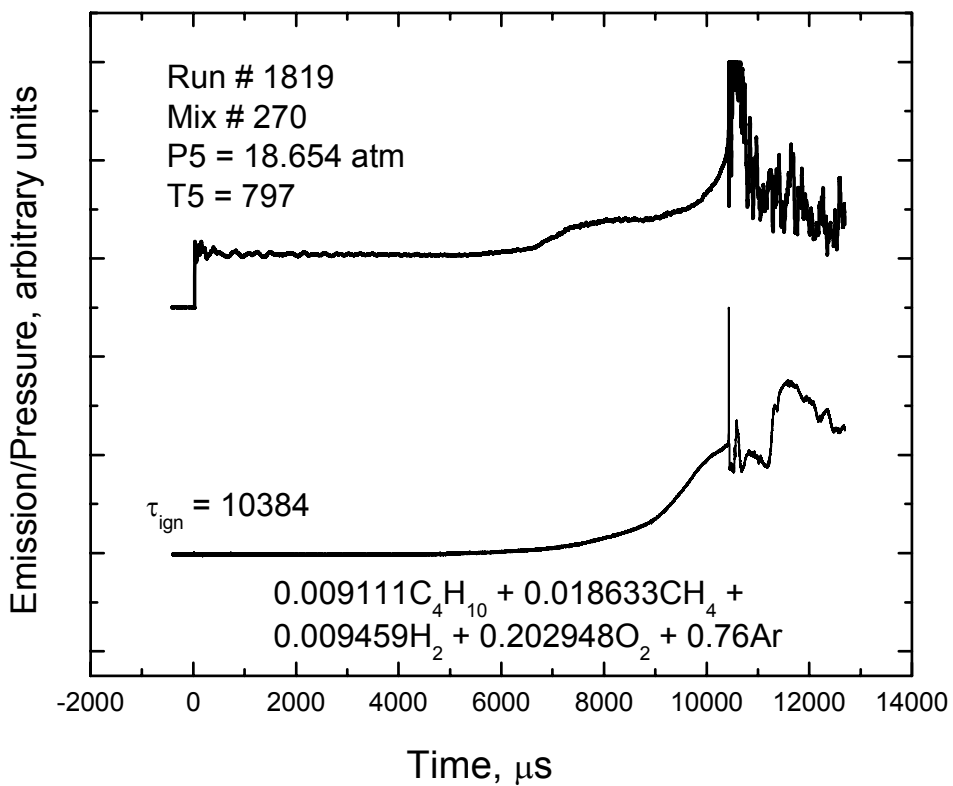
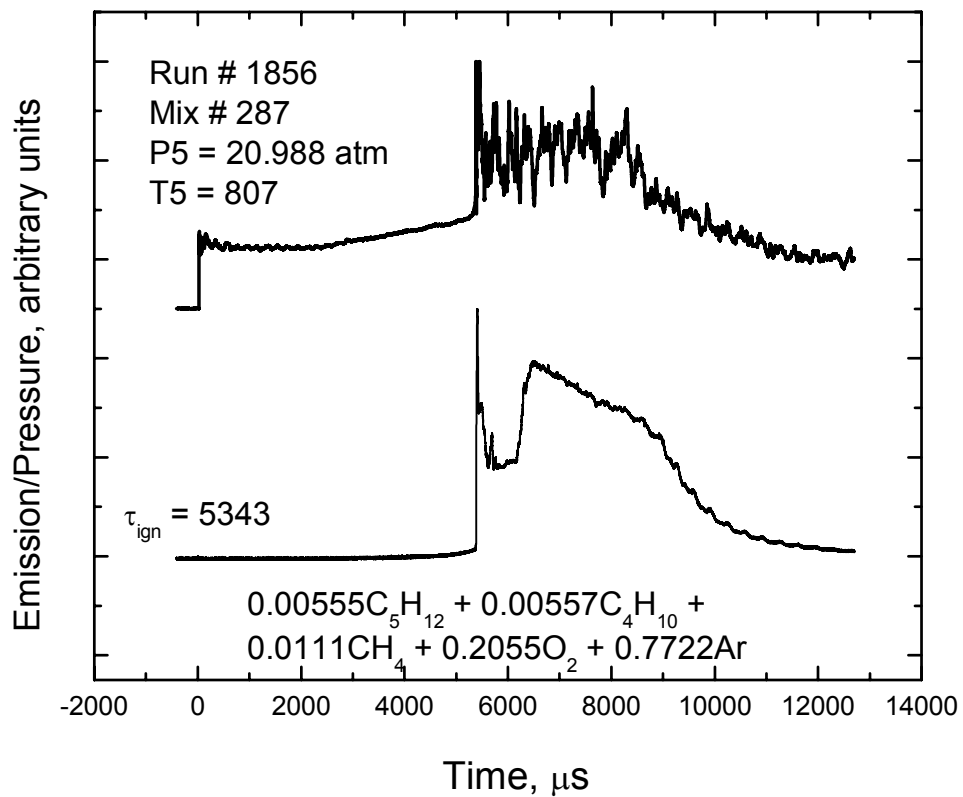


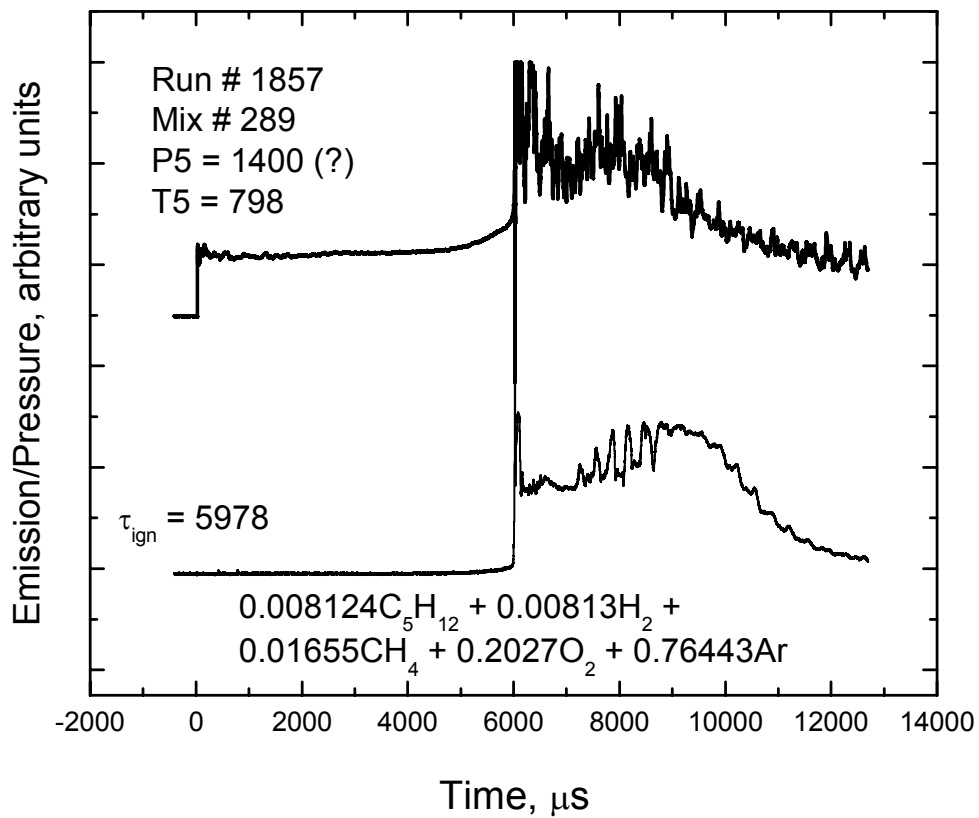
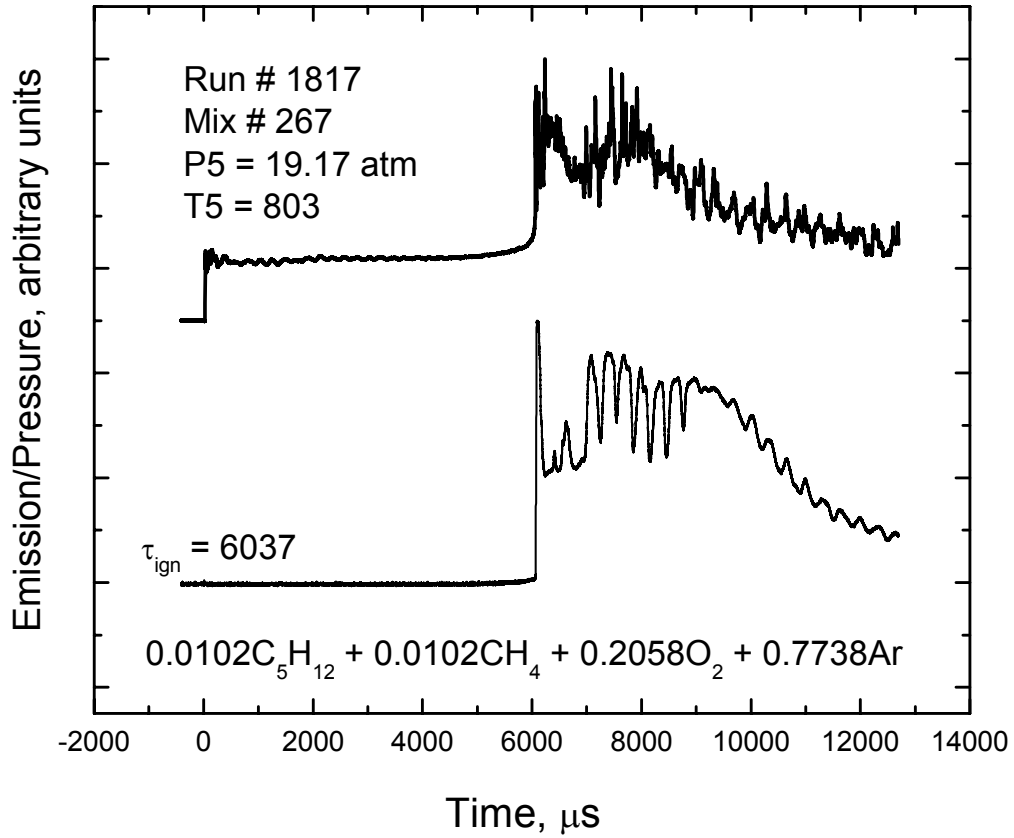


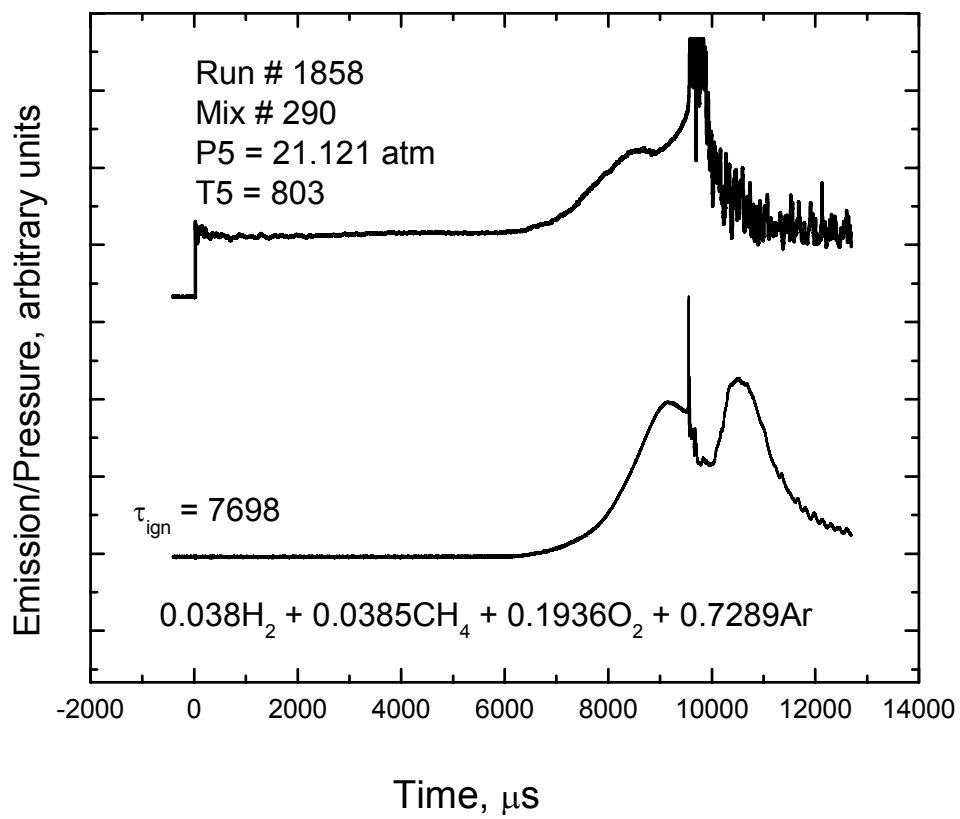












LIST OF REFERENCES

- [1] <http://www.eia.doe.gov>.
- [2] A. H Lefebvre, 1999, "Gas Turbine Combustion," 2nd Ed, Taylor & Francis, Philadelphia PA.
- [3] Environmental Protection Agency, 1993 "Alternate Control Techniques Document—NOx Emissions from Stationary Gas Turbines," Report No. EPA-453/R-93-007.
- [4] L. J. Spadaccini, and M. B. Colket, 1994, "Ignition Delay Characteristics of Methane Fuels," *Prog. Energy Combust. Sci.*, **20**, pp. 431-460.
- [5] J. de Vries, J. M. Hall, A. R. Amadio, E. L. Petersen, M. W. and Crofton, 2005, "Reflected-Shock Ignition of CH₄/C₂H₆/Air Fuel Blends," *Proc. of the 4th Joint Meeting of the US Section of the Combust. Inst. Philadelphia, PA.*
- [6] J. de Vries, J. M. Hall, M. W. Crofton, and E. L. Petersen, 2005, "A Shock Tube Study of CH₄/C₂H₆ and CH₄/C₃H₈ Fuel Blends Under Gas Turbine Conditions," *The 25th Int. Symp. On Shock Waves, Bangalore, India.*
- [7] E. L. Petersen, and J. de Vries, 2005, "Measuring the Ignition of Fuel Blends Using a Design of Experiments Approach," *AIAA Paper 2005-1165.*
- [8] J de Vries, and E. L. Petersen, 2005, "Toward a Reduced DOE Matrix for the Combustion of Gas Turbine Fuel Blends" *AIAA Regional Student Conference (Region II), Gainesville, FL.*
- [9] J. de Vries, E. L. and Petersen, 2005, "Design and Validation of a Reduced Test Matrix for the Autoignition of Gas Turbine Fuel Blends," *2005 ASME Int. Mech. Eng. Congress and Exposition, IMECE2005-80040, Orlando, FL.*

- [10] J. A. Cornell, 1990, "Experiments With Mixtures," 2nd Ed. Wiley series in probability and mathematical statistics. New York, NY.
- [11] E. L. Petersen, and M. W. Crofton, 2003 "Measurements of High-Temperature Silane Pyrolysis Using SiH₄ IR Emission and SiH₂ Laser Absorption," J. Phys. Chem. A, **107**, (50), pp. 10988-10995.
- [12] P. J. Ross, 2000, "Taguchi Techniques for Quality Engineering," McGraw-Hill, New York.
- [13] R. M. Myers. and D. C. Montgomery, 2002, "Response Surface Methodology," 2nd Ed. Wiley series in probability and mathematical statistics. New York, NY.
- [14] E. L. Petersen, M. J. A. Rickard, M. W. Crofton, E. D. Abbey, M. J. Traum, and D. Kalitan, M., 2005, "A Facility for Gas- and Condensed-Phase Measurements Behind Shock Waves," Meas. Sci. Technol., **16**, pp 1716-1729.
- [15] H. K. Ciezki and G. Adomeit, 1993, "Shock-Tube Investigation of Self-Ignition of n-Heptane-Air Mixtures under Engine Relevant Conditions," Combust. Flame, **93**, pp 421-433.
- [16] K. Fieweger, R. Blumenthal, and G. Adomeit, 1997, Self-Ignition os S.I. Engine Model Fuels: A Shock-Tube Investigation at High Pressures," Combust. Flame, **109**, pp 599-619.
- [17] H. J. Curran, P. Gaffuri, W. J. Pitz, and C. K. Westbrook, 1998, "A Comprehensive Modeling Study of n-Heptane Oxidation," Combust. Flame, **114**, pp 149-177.
- [18] E. L. Petersen, D. F. Davidson, and R. K. Hanson, 1999, "Kinetics Modeling of Shock-Induced Ignition in Low-Dilution CH₄/O₂ Mixtures at High Pressures and Intermediate Temperatures," Combust. Flame, **117**, pp 272-290.

- [19] R. Sierens and E. Rosseel, 2000, "variable Composition Hydrogen/Natural gas Mixtures for Increased Engine Efficiency and Decreased Emissions," *ASME J. Eng. Gas Turbines Power*, **122**, pp 135-140.
- [20] H. J. Curran, P. Gaffuri, W. J. Pitz, and C. K. Westbrook, 2002, "A comprehensive Modeling Study of iso-Octane Oxidation," *Combust. Flame*, **129**, pp 253-280.
- [21] N. Lamoureux and C. E. Paillard, 2003, "Natural Gas Ignition Delay Times Behind Reflected Shock Waves: Application to Modeling and Safety," *Shock Waves*, **13**, pp 57-68.
- [22] J. Huang, P. G. Hill, W. K. Bushe, and S. R. Munshi, 2004, "Shock-Tube Study of Methane Ignition under Engine-Relevant Conditions: Experiment and Modeling," *Combust. Flame*, **136**, pp 25-42.
- [23] R. M. Flores, V. G. McDonell, G. S. Samuelsen, 2003, "Impact of Ethane and Propane variation in Natural Gas on the Performance of a Model Gas Turbine Combustor," *ASME J. Eng. Gas Turbines Power*, **125**, pp 701-708.
- [24] R. M. Flores, M. M. Miyasato, V. G. McDonell, G. S. and Samuelsen, 2001, "Response of a Model Gas Turbine Combustor to Variation in Gaseous Fuel Composition," *ASME J. Eng. Gas Turbines Power*, **123**, pp. 824-831.
- [25] A. El Bakali, P. Dagaut, L. Pillier, P. Desgroux, J. F. Pauwels, A. Rida, and P. Meunier, 2004, "Experimental and Modeling Study of the Oxidation of Natural gas in a Premixed Flame, Shock Tube, and Jet-Stirred reactor," *Combust. Flame*, **137**, pp 109-128.
- [26] B. M. Gauthier, D. F. Davidson, and R. K. Hanson, 2004, "Shock Tube Determination of Ignition Delay Times in Fuel-Blend and Surrogate Fuel Mixtures," *Combust. Flame*, **139**, pp 300-311.

- [27] V. P. Zhukov, V. A. Sechenov, and A. Yu. Starikovskii, 2005, "Self-Ignition of a Lean Mixture of n-Pentane and Air over a wide range of Pressures," *Combust. Flame*, **140**, pp 196-203.
- [28] J. Herzler, L. Jerig, and P. Roth, 2004, "Shock-Tube Study of the Ignition of Propane at Intermediate Temperatures and High Pressures," *Combust. Sci. and Tech.* **176**, pp 1627-1637.
- [29] J. Herzler, L. Jerig, and P. Roth, 2005, "Shock Tube Study of the Ignition of Lean n-Heptane/Air Mixtures at Intermediate Temperatures and high Pressures," *Proc. Combust. Int.* **30**, pp 1147-1153.
- [30] F. Buda, R. Bounaceur, V. Warth, P. A. Glaude, R. Fournet, and F. Battin-Leclerc, 2005, "Progress Toward a Unified Detailed Kinetic Model for the Autoignition of Alkanes from C₄ to C₁₀ Between 600 and 1200 K," *Combust. Flame*, **142**, pp 170-186.
- [31] J. Huang and W. K. Bushe, 2005, "Experimental and Kinetic Study of Autoignition in Methane/Ethane/Air and Methane/Propane/Air Mixtures under Engine Relevant Conditions," *Combust. Flame*, in press.
- [32] Pratt & Whitney, 1992, Pratt & Whitney Workshop in Taguchi/Statistical Design of Experiments Methods.
- [33] G. E. P. Box and D. W. Behnkin, 1960, "Some New Three Level Designs for the Study of Quantitative Variables," *Technometrics*, **2**, (4), pp. 455-475.
- [34] R. J. Kee, F. M. Rupley, J. A. Miller, M. E. Coltrin, J. F. Grcar, E. Meeks, H. K. Moffat, A. E. Lutz, G. Dixon-Lewis, M. D. Smooke, J. Warnatz,, G. H. Evans, R. S. Larson, E. Mitchell, L. R. Petzold, W. C. Reynolds, M. Caracotsios, W. E. Stewart, P. Glarborg, C.

- Wang, O. Adigun, 2000, *Chemkin Collection*, Release 3.6, Reaction Design, Inc., San Diego, CA.
- [35] E. L. Petersen, D. F. Davidson, R. K. and Hanson, 1999, "Ignition Delay Times of Ram Accelerator CH₄/O₂/Diluent Mixtures," *J. Prop. Power*, **15**, (1) , pp. 82-91.
- [36] E. L. Petersen, J. M. Hall, S. D. Smith, J. de Vries, A. R. Amadio, and M. W. Crofton, 2005, "Ignition of Lean Methane-Based Fuel Blends at Gas Turbine Pressures," *Proc. ASME Turbo Expo: Power for Land, Sea and Air*, GT2005-68517, Reno, NV, USA.
- [37] C. T. Bowman and R. K. Hanson, 1979, "Shock tube measurements of rate coefficients of elementary gas reactions," *J. Phys. Chem.* **83**, pp 757-763.
- [38] I. I. Glass and J. P. Sisljan, 1994, "Non Stationary Flows and Shock Waves," (Oxford: Clarendon).
- [39] K. A. Bhaskaran and P. Roth, 2002, "The shock tube as wave reactor for kinetic studies and material systems," *Prog. Energy Combust. Sci.* **28**, pp 151-192.
- [40] H. W. Liepman and A. Roshko, 1985, "Elements of Gasdynamics," Dover Publications, INC. Mineola, New York.
- [41] Ya. B. Zel'dovich and Yu. P. Raizer, 2002, "Physics of Shock Waves and High – Temperature Hydrodynamic Phenomena," Dover Publications, INC. Mineola, New York.
- [42] J. D. Anderson, Jr., 2003, "Modern Compressible Flow With Historical Perspective," 3rd Ed., McGraw-Hill, New York, NY.
- [43] I. I. Glass and J. P. Sisljan, 1994, "Nonstationary Flows and Shock Waves," Oxford University Press Inc., New York, NY.

[44] A. R. Amadio, J. de Vries, J. M. Hall, and E. L. Petersen, 2005, "Driver-Gas Tailoring for Low-Temperature Chemical Kinetics," Proceedings of the 4th Joint Meeting of the U.S. Sections of The Combustion Institute, Philadelphia, PA.

[45] A. R. Amadio, E. L. Petersen, and M.W. Crofton, 2005, "Driver-gas tailoring for chemical kinetics experiments using unconventional driver mixtures," 25 International Shock-Wave Symposium, Bangalore, India.